TECHNICAL REPORT

ON THE INTERPRETATION OF FETCH-LIMITED WAVE SPECTRA AS MEASURED BY AN AIRBORNE SEA-SWELL RECORDER

T. P. BARNETT
Exploratory Oceanography Division
J. C. WILKERSON
Oceanographic Prediction Division

MAY 1967

ABSTRACT

A section of sea surface that had been subjected to a constant, offshore wind was profiled using an airborne radar wave profiler.   The profiles extended from the coast out to a distance of 190 nautical miles.   From this data estimates of the spectrum of encounter of the sea surface were obtained for a number of different fetch lengths.   By solving a singular Fredholm integral equation of the first kind, it was possible to retrieve the true wave spectrum as a function of fetch length. Spectral growth curves were then obtained and analyzed in light of recent theories of wave generation.   The data lend support to the previous conclusions of Snyder and Cox (1966) regarding two recent theories of wave generation.   Specifically, the data are consistent with the "resonance" theory of wave growth (Phillips, 1957), but at the same time suggests that wave growth through an instability mechanism (Miles, 1957) is yet to be understood.   It is also demonstrated that energy is transmitted simultaneously to the entire frequency range of the wave spectrum.   One of the most significant results of this study was that higher frequency waves grew past or "over-_____. After "over-_____an equilibrium

FOREWORD

There has been intense interest in the exact mechanisms by which wind energy is converted to wave energy since Sverdrup and Munk originally postulated their wave prediction theory in 1943. Nevertheless, there has been a dearth of carefully collected data on the actual growth of wind waves. The initial attempt to observe this wave growth from the air was made in 1946 by the United Kingdom's Admiralty Research Laboratory using a downward looking radio altimeter flying over the Irish Sea. Subsequent attempts in both the United Kingdom and the United States to duplicate this original experiment were without success until 1964, when the Naval Oceanographic Office, using the specially equipped oceanographic aircraft of the Navy's Oceanographic Air Survey Unit based at Patuxent Naval Air Station, Maryland, began to obtain excellent wave profiles.

Working with the officers and men of the Oceanographic Air Survey Unit, Dr. T. P. Barnett and Mr. J. C. Wilkerson of the Naval Oceanographic Office planned and implemented special wave-spectra measuring flights starting in 1965 to take advantage of this long-needed capability to profile the sea surface from the air. The resolution of the continuous vertical profile is of the order of one foot in the vertical and 100 feet in the horizontal. Once these truly unique field data were at hand, the authors were able to analyze in depth the validity of various theories now existent regarding wave generation and dissipation. The authors' efforts have been most successful in this regard, and their study can be considered one of the outstanding contributions during this decade in this still growing field of airborne oceanography.

L. E. DeCamp

L. E. DECAMP
Captain, U. S. Navy
Commander
U. S. Naval Oceanographic Office

ACKNOWLEDGEMENTS

TABLE OF CONTENTS

TABLE OF CONTENTS (Continued)

FIGURES

FIGURES (Continued)

Page

TABLES

1.0   INTRODUCTION

Why waves form when air flows over water is a question about nature which has not yet been satisfactorily answered. This is no fault of the theoreticians, however, for several theories that could account for wave generation have been advanced. The real problem is that, with the exception of Snyder and Cox (1966), it has not been possible to observe adequately the manner(s) in which the wind actually adds energy to the wave spectrum. With this in mind, the U. S. Naval Oceanographic Office has initiated a series of field experiments designed to measure the rate of growth of the energy spectrum under steady wind conditions. This paper will describe the method and results of the first of these experiments.

The basic idea was to observe steady state, fetch-limited wave spectra that had been developed by a geophysically uniform wind field and that were representative of a number of different fetch lengths. From these observations it was possible to obtain estimates of spectral growth. In practice, the experiment was timed to take place after a strong low pressure system had passed over the East Coast of the United States and the offshore winds behind the frontal system had established a stationary wave system in the area within about 100 nautical miles of the coast. An aircraft, equipped with a high-resolution radar altimeter, was then sent aloft to obtain continuous profiles of the sea surface from the coast downwind to a desired distance. A similar run was made upwind. The data were subsequently transformed into spectra representative of various distances from the coast. These spectra eventually provided estimates of spectral growth over the major frequency range of the spectrum. A key issue in the analysis was that the wind field should have been constant during and for a given time before the flight. This requirement is treated at length in Section 4.

2.0   GENERAL THEORY AND BACKGROUND

The method employed in reducing the sea surface profiles, as seen from the plane, to the final estimates of real spectral growth will be discussed in later sections of this paper. For the moment attention is confined to a description of the general theoretical approach to and appropriate background information on the overall experiment.

Hasselmann (1960) and Groves & Melcer (1961) independently proposed the following general equation to describe the energy balance of the wave spectrum in deep water:

1

$$\frac{\partial F}{\partial t}(\sigma, \phi, \vec{x}, t) + \vec{V}_g(\sigma, \phi) \cdot \vec{\nabla}_{\vec{x}} F(\sigma, \phi, \vec{x}, t) = G(\sigma, \phi, \vec{x}, t) \qquad (1)$$

where $F(\sigma, \phi, x, t)$ is the local energy spectrum at position $\vec{x}$ and time t, $\vec{V}_g(\sigma, \phi)$ is the group velocity of the component with circular frequency σ and relative direction ϕ and the function $G(\sigma, \phi, \vec{x}, t)$ represents all processes which are adding to or subtracting energy from F. The complete G-function is not within the realm of present knowledge, but it is possible to define a linear form of G that will be adequate for our immediate purposes:

$$G(\sigma, \phi, \vec{x}, t) = \alpha(\sigma, \phi, \vec{x}, t) + \beta(\sigma, \phi, \vec{x}, t) \cdot F(\sigma, \phi, \vec{x}, t). \qquad (2)$$

α and β correspond to wave growth mechanisms that are linear and exponential, respectively, in time (space). Such mechanisms might, respectively, be explained by the "resonance theory" of Phillips (1957) and the shear-flow theory of Miles (1957). Reviews of these theories are given in the literature (e.g. Longuett-Higgins, et al., 1963) and will not be repeated here. Equation (1) then is the linear form of the energy equation with G given by (2) and will be considered valid until non-linear and/or dissipative effects take over.

It is clear that an appropriate form of equation (1) can be used to obtain estimates of α and β provided it is possible to fulfil one of three conditions during the initial growth phase:

(i) $F(\sigma, \phi, \vec{x}, t)$ and $\vec{W}(\vec{x}, t)$ known for sufficient t and $\vec{x}$,

(ii) $F(\sigma_o, \phi_o, t)$ and $\vec{W}(\vec{V}_g t, t)$ known for sufficient t and $\vec{V}_g$ equal the group velocity of the σ_o, ϕ_o component,

(iii) $F(\sigma, \phi, \vec{x})$ and $\vec{W}(x)$ known for sufficient $\vec{x}$ and stationary for specified t.

The first condition essentially estimates α and β by a hindcasting technique and generally involves the solution of a nonlinear integro-differential form of equation (1). Details of such an analysis are presented by Barnett, 1966.

The second circumstance is identical to the case considered by Snyder (1965) and summarized in Snyder & Cox (1966). In this experiment a series of wave recorders was towed at constant speed downwind from the lee of Eleuthera Island in the Bahamas. As observed by the moving recorders, a singularity in the spectral transformation relating the true frequency and direction of the wave to its apparent frequency and direction allowed an estimate of the intensity of a single spectral component. This component had a group velocity equal to the towing velocity. Spectral growth curves were

obtained for this single, fixed frequency component over a range of wind speeds. From these data it was possible for the first time to evaluate quantitatively the relative importance and correctness of the wave growth theories previously mentioned. The results supported the resonance theory of Phillips. They also showed that the instability theory of Miles predicted rates of wave growth that were almost an order of magnitude too low.

The final condition is the one met by this work. Expanding on (iii), it is sufficient that the wind field be at least weakly stationary over a reasonably large region that encompasses the locations at which observations are to be made. The amount of time, t, during which the wind should have been stationary depends on the frequency component to be observed and the fetch distance at which the observation is to be made. This quantity may be approximated by the equation

$$t = \frac{d}{V_g\,(\sigma\,)} \tag{3}$$

with d equal to the maximum fetch distance for which the σ-component would be fully developed and both d and t $\gg$ 0 (Phillips, 1958a). For all frequencies which satisfy (3) whose time for full development is less than that given by (3) with d and σ given, equation (1) reduces to:

$$\vec{V_g}\,(\sigma,\phi)\,\cdot\,\vec{\nabla}_{\overrightarrow{x}}\,F\,(\sigma,\,\phi\,\overrightarrow{x}) = G\,(\sigma,\phi,\overrightarrow{x}). \tag{4}$$

By considering only the steady state fetch limited case, we have reduced the data necessary to evaluate α and β to F ($\sigma,\phi,\overrightarrow{x}$) and $\vec{W}\,\overrightarrow{(x)}$. Without the aid of an inordinate number of ships and/or oceanographic buoys, collection of even these data would seem a formidable and, in fact, nearly impossible task. However, the relatively fast (200 knot) airplane-altimeter arrangement provides an estimate of F ($\sigma,\phi,\overrightarrow{x}$), and by working with uniform wind fields $\vec{W}\,\overrightarrow{(x)}$ is reduces to $\vec{W}$. Both of these simplifications involve certain assumptions that will be justified in later sections.

It is appropriate here to compare the work of Snyder and Cox (1966) with the present effort. Both experiments are similar in their intent and approach. Both obtain their raw data from a moving platform and hence have their theoretical base in the work of St. Denis and Pierson (1953) and Cartwright (1963). Both eventually arrive at a final estimate of spectral growth. These estimates are logically compared by both sets of authors against the predictions of various theories. Here the similarity ends. Snyder and Cox observe, with relatively good accuracy, the growth of a single frequency component over a range of wind speeds. On the other hand this work observes simultaneously the growth of a number of frequency components under a single wind condition. The two sets of measurements essentially represent the Eulerian and LaGrangian view points. Also dissimilar is the way in which the final estimates of spectral growth are

3

obtained: In the first case new time series concepts were developed, and in the second a Fredholm integral equation of the first kind is solved. Both approaches are complimentary in that the strong points of one generally tend to compensate for the weaknesses of the other, and comparisons of final results, where possible, are reinforcing.

3.0   INSTRUMENTS

3.1   Sea Surface Profiler

The airborne radar wave profiler used in this experiment is an advanced system being developed for the U. S. Naval Oceanographic Office by AMECOM Division of Litton Systems, Inc. It is composed of three functional sections: the antenna assembly, height sensor, and vertical aircraft motion sensor. Figure 1 shows a simplified block diagram of the instrument and Table 1 lists its more important characteristics.

The antenna assembly is a single, parabolic reflector using the "Split Feed with Septum" technique which permits the single antenna to function simultaneously as a transmitting antenna on the one half and a receiving antenna on the other. The assembly is mounted very near the center of gravity of the aircraft (a Lockheed Super Constellation).

Vertical motion of the aircraft is sensed by an accelerometer (range $\pm 1g$, sensitivity $0.0001g$), which provides a signal to electronic circuitry where double integration takes place. The output is representative of aircraft displacement and is applied as a second input to a summing network. With proper scaling factor and phasing, this signal cancels the incremental altitude signal input created by the vertical displacement of the aircraft. All other signals (wave height information) from the summing network are then forwarded to a precise, fixed gain voltage amplifier, the output of which is recorded on an oscillograph. Figure 2 shows an analog trace of the outputs of the wave height sensor and the doubly integrated accelerometer signal.

At the operating altitude of 500 feet, the antenna illuminates a circular spot on the sea surface approximately 15 feet in diameter. Theoretically, this places the limit of wave length resolution at 30 feet. In actual practice, however, the system noise level is unacceptable when operating with an instrument response time (.01 second) fast enough to match the minimum wave length resolution possible with the antenna. It was decided that the present experiment would concern itself with wave lengths greater than 100 feet, hence, the response time of the system was decreased to 0.1 second. This value effected removal of most of the high frequency noise components in the frequency band of apparent wave intelligence.
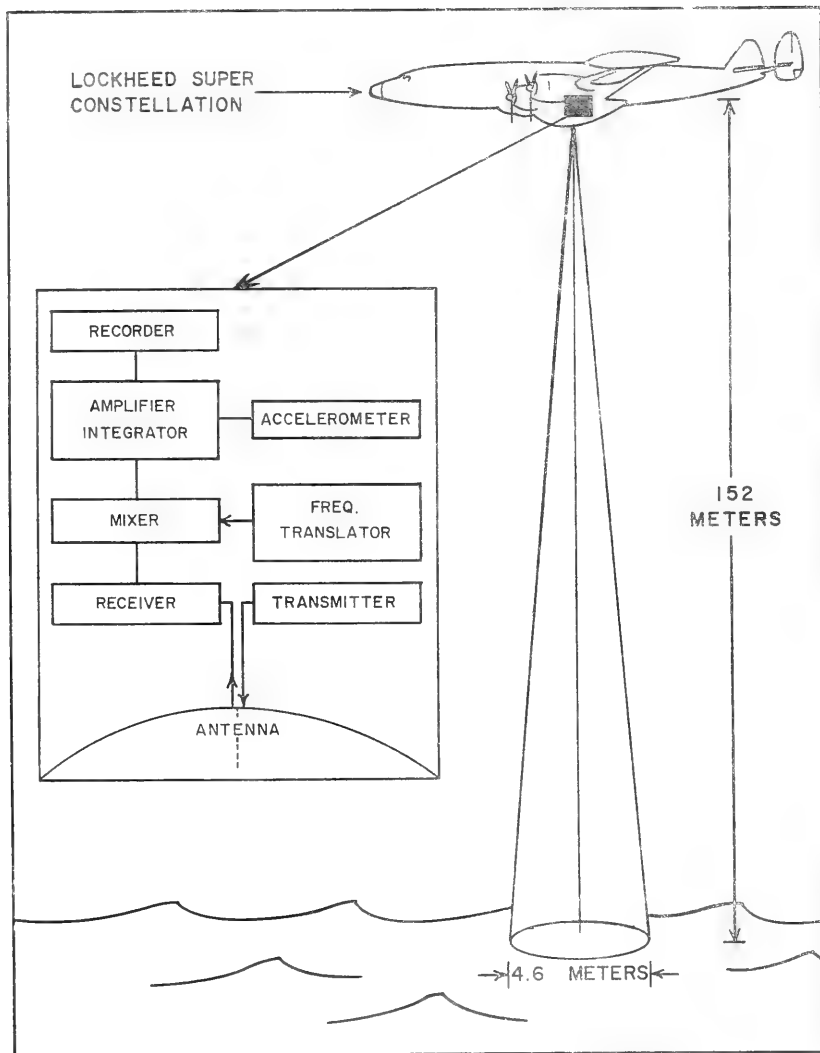
FIGURE 1. A SCHEMATIC VIEW OF THE AIRBORNE
SEA SURFACE PROFILER.

TABLE I

PERFORMANCE CHARACTERISTICS OF THE
AMECON WAVE HEIGHT INDICATOR

Frequency	4300 mc
Modulation - FM	25 kc
Power Output	300 mw
Antenna	Split Parabola
Beam Width	1.72°
Nominal Operating Altitude	500 ft.
Accuracy	Wave height between 2 and 50 feet, ± 10% of actual value or 0.5 feet, whichever is greater
Resolution	Wave lengths from 30 - 2000 feet
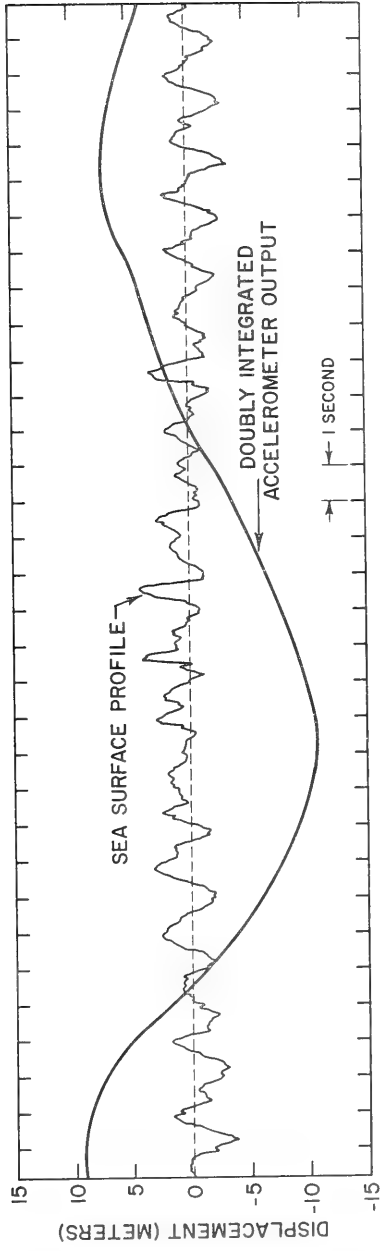
FIGURE 2. A TYPICAL LENGTH OF PROFILER RECORD.

7

A performance test of the airborne wave profiler was conducted at Argus Island Tower, Bermuda several years ago. While the aircraft took profiles of the sea surface along flight tracks directed up and downwind, wave measurements were being taken simultaneously at the Tower with a very accurate resistance-wire wave staff. The performance test began about 16 hours after the passage of a frontal system that had winds of speeds 30-35 knots and direction 280°T associated with it. The effective fetch was approximately 400 nautical miles. In short, measurements were made of what would commonly be described as a "fully developed", stationary and homogeneous wind sea.

Typical resulting comparisons of the energy spectrum of the sea surface as measured by the aircraft and wave staff are shown in Figure 3. Unfortunately, the comparison plane data was evaluated using only the assumption that all waves were travelling downwind. For wave frequencies higher than the frequency of the spectral peak, this is an unrealistic assumption and is one of the reasons for the underestimates in the mid-frequency range of the spectrum. A more general approach (section 6.0) using spectral spreading factors (section 5.2) that are more in line with observation would probably have yielded a better correspondence. It will be seen that by varying the assumed spreading factor one varies the magnitude of the spectral estimates but leaves the qualitative features unaltered (Section 7.1).

The comparisons of Figure 3 are considered quite good in the frequency range about the spectral maximum. As was expected, the agreement degraded with increasing wave frequency. While some of this was due to the unrealistic spreading factor, a larger portion was due to the system response used during the test. In an effort to minimize system noise, a relatively large time constant (0.19 sec) was used. In correcting the resulting spectra for instrument response, however, the small amount of noise that did remain combined with the large correction factors for higher frequency range. In the present study, as previously mentioned, a compromise response factor of 0.1 second was used. The relative instrument responses for the 0.19 and 0.10 second time constants are shown in Figure 4. In addition, system modifications were made, before the present experiment, that tangibly reduced the noise level. Unfortunately, as will be seen, the noise level was still high enough to provoke considerable uncertainty of relatively high frequency spectral estimates.

3.2   Aircraft Motions

Pitching, rolling, and heaving motions of the aircraft introduced unwanted noise to the wave profile. Of these three motions, the heaving motions were the most important due to their relative magnitude. As can be seen from the sample analog trace, vertical displacements approaching 25 meters were recorded. Cancellation of the relatively high frequency vertical motion by the doubly integrated accelerometer output appears nearly complete. Some error resulted from the practical limits to which
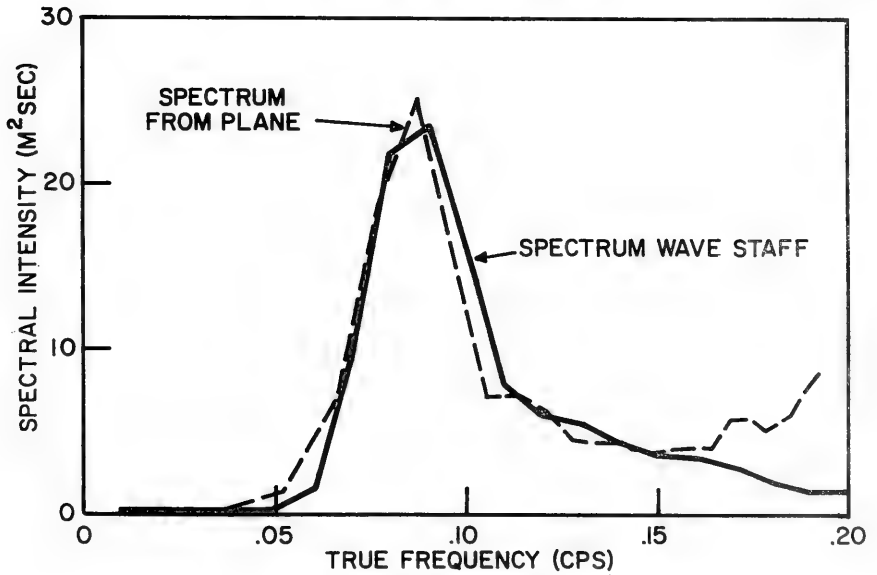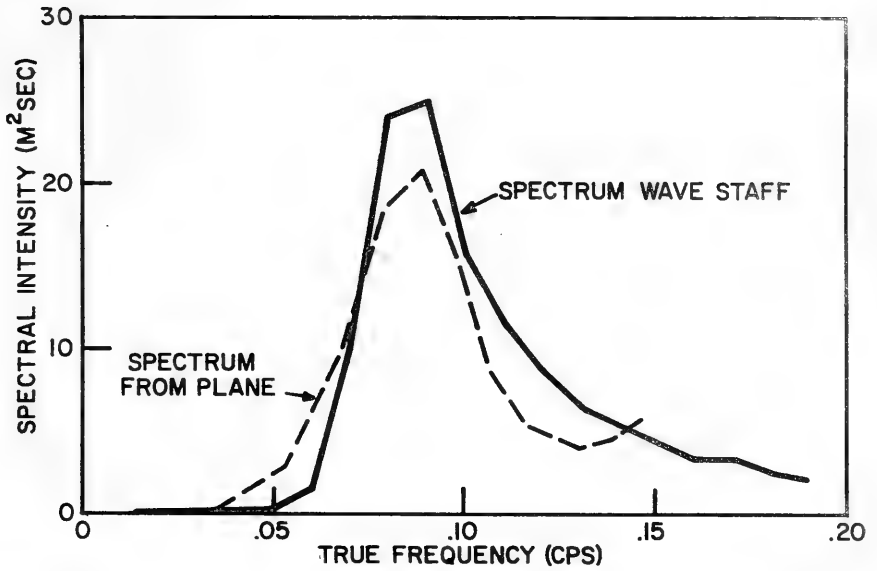
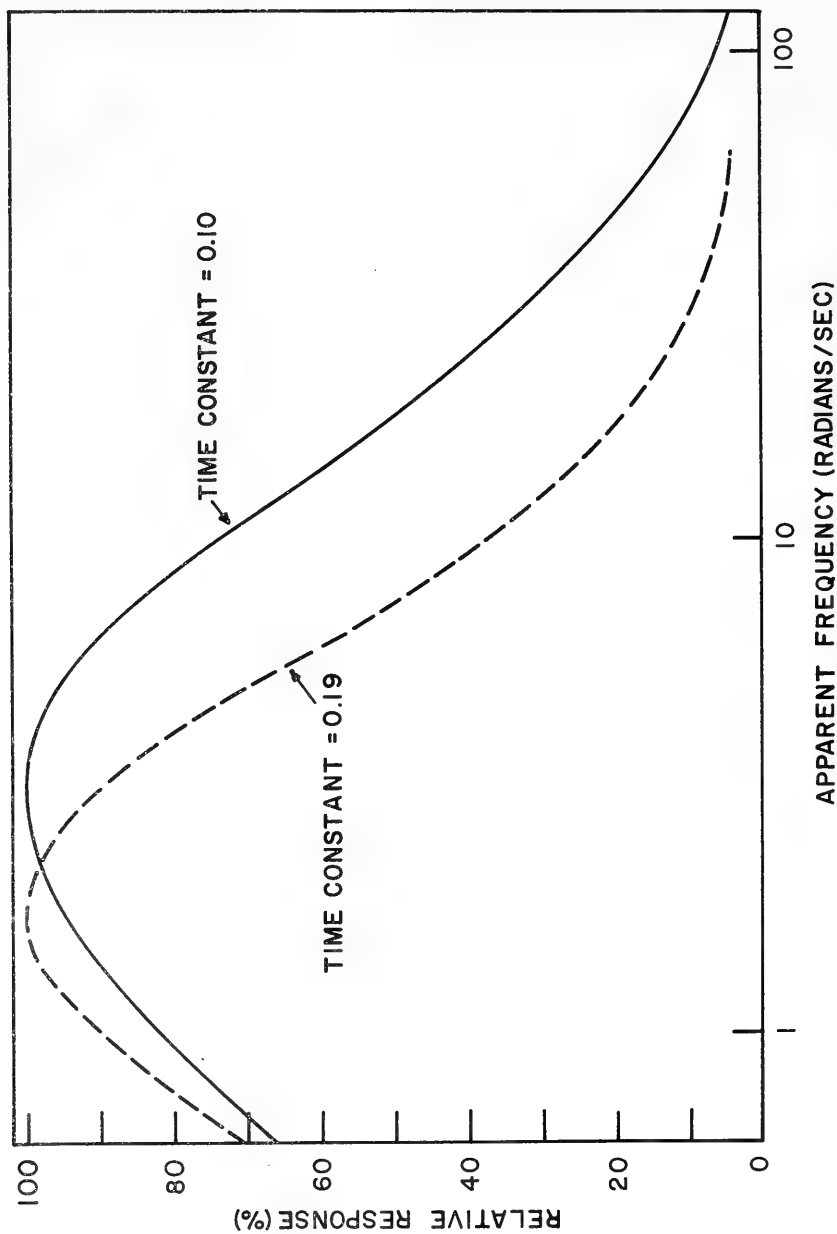FIGURE 3. COMPARISON OF WAVE STAFF AND PLANE SPECTRA.

9

FIGURE 4. FREQUENCY RESPONSE OF THE AIRBORNE SEA SURFACE PROFILER SYSTEM.

10

the scale factors of the wave height sensor and the vertical motions sensor can be made equal. This error appears in the recording as a very low amplitude noise of a period identical to the period of vertical motion of the aircraft. From the sample of Figure 2, this period appears to be about 30 seconds and corresponds to a wave length of 2,800 meters, well outside the range of interest.

While it is informative to investigate the magnitude of the errors introduced by pitching and rolling of the plane, it is more to the point to ask if these errors are, in fact, introduced at all. The performance tests discussed in the previous section would seem to indicate that the plane motions do not significantly affect the results. To investigate this question further, time histories of pitch and roll angles were obtained under turbulent atmospheric conditions, conditions quite similar to those under which the data presented in this paper were taken. These estimates of pitch and roll angles came from the dip angle indicator of a fixed airborne magnetometer*. If the plane heading is either magnetic east or west, the variation of dip angle, as seen by the fixed magnetometer, is essentially a measure of the rolling motion of the aircraft. If the plane is heading either magnetic north or sourth, the variation in dip angle is a measure of the pitching motion. Two typical power spectra of these time series were computed (Section 5.1) and are shown in Figure 5. Clearly the majority of the energy in these spectra is associated with quite low frequencies. It will turn out that these frequencies are well below those at which common wind generated gravity waves appear to occur. Further, these measurements show that even under very turbulent conditions, mean values of the roll angle are less than one degree (.02 radians). Maximum roll angles are under 3 degrees. These same measurements indicate also that pitch angles are usually much less than roll angles. It can be shown that even with roll or pitch angles of 3 degrees, the error in apparent wave height is less than .7 meters.

Unfortunately, it was not possible to monitor the pitch and roll angles of the aircraft during this experiment. In flight, however, automatic control, through the auto-pilot system, corrected all rotational motions greater than 0.25 degrees of angle, which is the minimum level of sensitivity of its servo mechanisms. Although the lag time of the entire control system would necessarily result in angles greater than 0.25 degrees, it seems quite reasonable to assume that these angles were certainly less than 3 degrees.
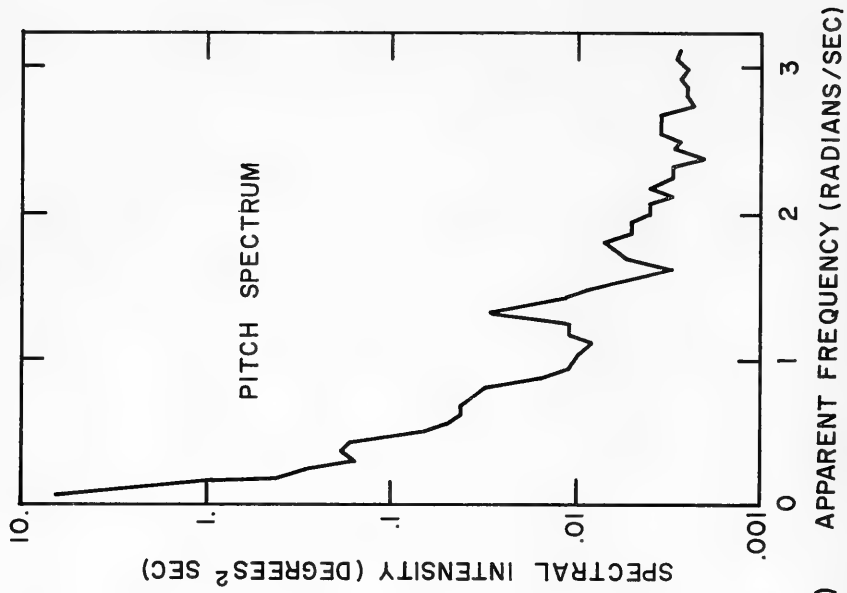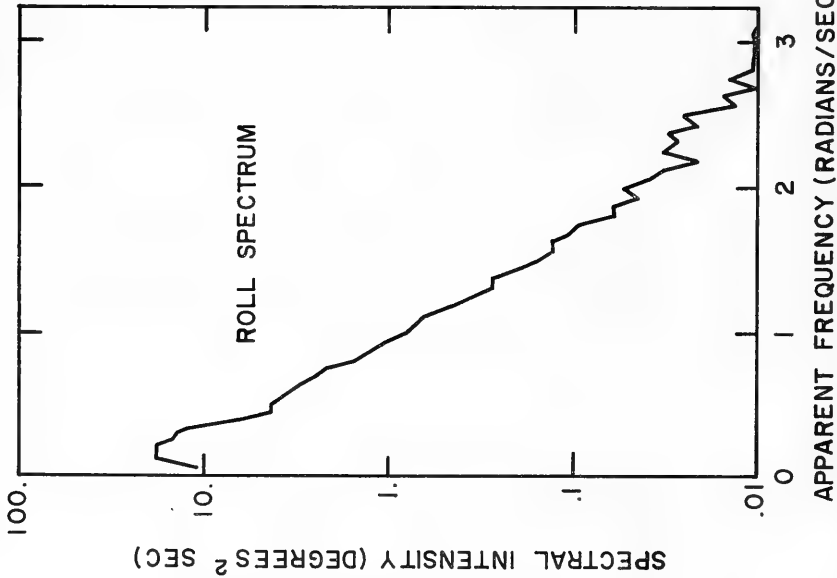
FIGURE 5. TYPICAL POWER SPECTRA OF AIRCRAFT PITCH AND ROLL MOTIONS.

12

It is apparent that the measurements taken during this experiment have not been seriously affected by the various motions of the aircraft. Nevertheless, plans are being made to record the rotational motions of the aircraft in all subsequent work.

3.3 Navigation

Navigation of the aircraft was accomplished with LORAN A. After an initial positioning over the TACAN Station at Sea Isle, New Jersey, lines of position were determined from LORAN rates 1H4 and 1H5. Estimates of positioning error are shown in Figure 6 which contains accuracy contours for these two rates at the 95% confidence level. It is clear that estimates of positioning can be approximated no more accurately than ±0.5 nautical mile at the 95% level. This estimate of accuracy is based on the assumption that other contributing factors such as operator error and instrument calibration error (for both airborne and ground equipment) were negligible. While the assumption of negligible instrument error is reasonably sound, the same may not always be said for operator error which depends, among other things, on operator skill and quality of the LORAN signal. Errors in heading are related to errors in lines of position since individual changes in heading were based on each of the points of position. It appears that estimates of plane heading may be considered accurate to within 5°.

4.0 THE WEATHER SITUATION

4.1 The General Weather Picture

In order to attempt significant estimates of the evolution of wave spectrum, it was essential, as previously noted, that the measurements be made under "ideal" wind conditions. Ideal, in this case, meant that an offshore wind of constant velocity should have been blowing over a large area of ocean for a time t (Section 2.0) prior to wave observation. Further, it was required that the wind field should have been uniform in its lateral extent. These were rigorous conditions to try to meet, but quite fortunately the wind field over and around the area of measurement was about as geophysically constant as could be hoped.

The general weather situation was as follows*: Early on 17 February a weak low pressure system (1007 mb) located just north of the North Dakota-Canadian border began to develop further in its eastward movement. A high pressure system of moderate strength pushing ESE out of Canada was beginning to accelerate the eastward movement of the cyclone. At 0000Z on 18 February, the now massive cyclone center (1000mb) was located midway between James Bay and the Great Lakes.

*We are grateful to Mr. Lionel I. Moskowitz for providing the general weather analysis.
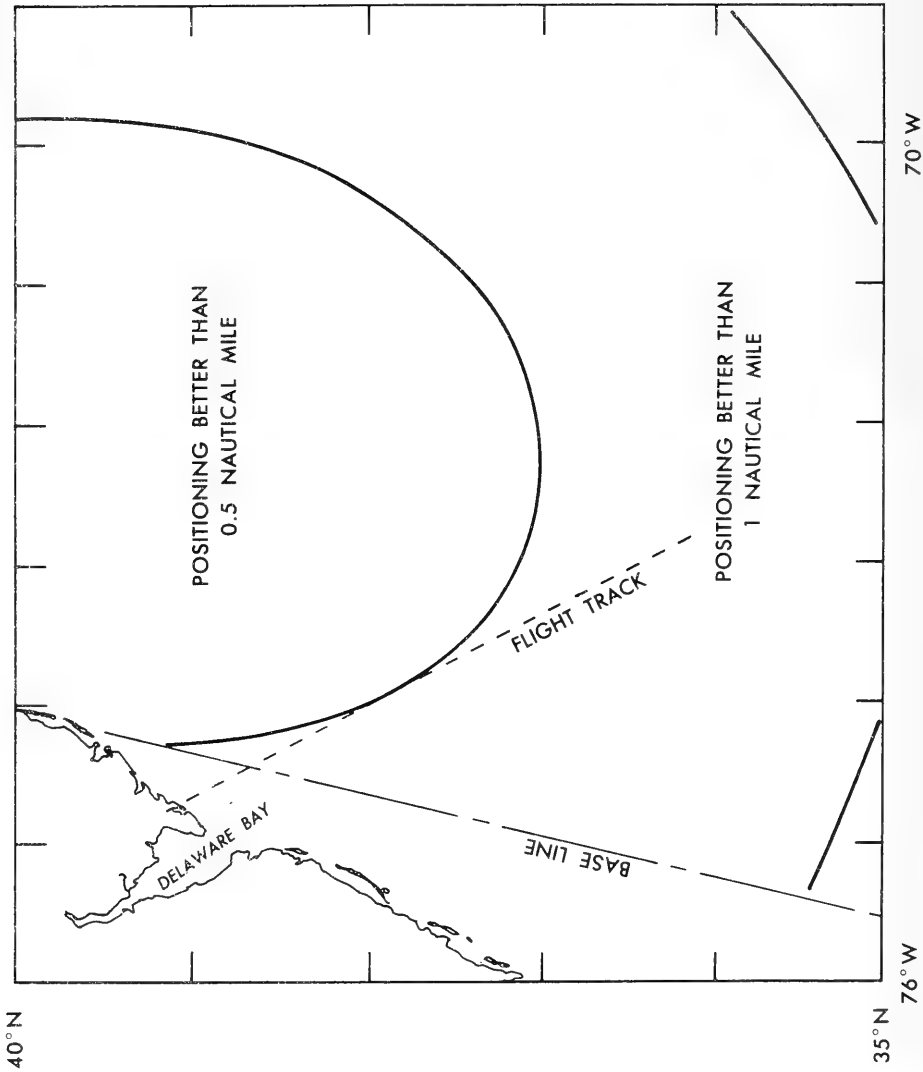
13

POSITIONING BETTER THAN
0.5 NAUTICAL MILE

POSITIONING BETTER THAN
1 NAUTICAL MILE

FLIGHT TRACK

BASE LINE

DELAWARE BAY

40° N

35° N

76° W

70° W

FIGURE 6. 95% ACCURACY CONTOURS FOR 2-LINE POSITIONING
USING LORAN-A RATES 1H4 AND 1H5.

14

A north-south isobaric configuration, with practically no field curvature, developed to the west of the cyclone center and was maintained till after 1200Z on 20 February. The coastal winds off the Mid-Atlantic states were light (10-15kts) and variable until the frontal system passed the coast (0000Z, 19 February). The cyclone began to rapidly intensify after passing over New England. The center fell to 984 mb at 0000Z on 20 February. The deepening of the cyclone led to an intensification of the pressure gradient which increased surface wind speeds behind the frontal system. These winds affected the coastal areas from Maine to Cape Hatteras, N. C.

4.2   A Closer Look at the Wind Field

The National Weather Records Center in Ashville, N. C. was able to supply enough additional data to allow a more detailed look at the structure of the wind field. These data are presented in Figure 7. The notation "A" at the base of an arrow indicates the data were taken with an anemometer. All anemometer winds at sea were gathered by lightships and have been reduced to an equivalent 10 meter wind assuming a logarithmic profile and the drag coefficient data of DeLeonibus (in preparation). This 10 meter height corresponds to the same level that visual estimates taken from shipboard are purported to represent. It was not worthwhile to similarly reduce winds taken at land stations for obvious reasons. Considering the many different ships reporting, the winds were remarkably uniform. A wind speed of 30-35 kts (15.4 - 18.0 m/sec) and direction of 335°T is typical of the values reported. The plane track is shown on each map and was essentially oriented parallel to the wind direction.

The relative steadiness of the wind field is apparent from an inspection of the above illustrations. In addition, Figure 8 shows a time history of the wind force and direction at selected near shore stations where anemometers were used. Since the data were only available in terms of Beaufort force, no attempt has been made to correct for different anemometer heights. However, all of the anemometers were at a height of 18 to 19.5 meters above the sea surface, so the data were taken at essentially the same elevation. Since the air mass associated with this storm was very unstable*, it is to be expected that some variability due to gustiness will be present in these figures. Even with this variability the constancy of the nearshore wind field through the measurement time was reasonably good.

It was not possible to obtain similar anemometer wind information for the region far from shore. However, estimates of the wind in this area through accurate plane positioning were obtained. By locating the plane every five minutes via LORAN A (Section 3.3), the ground speed was estimated. Since the true air speed

*Air-sea temperature differences as reported by the light ships were between -6° and -10°C.
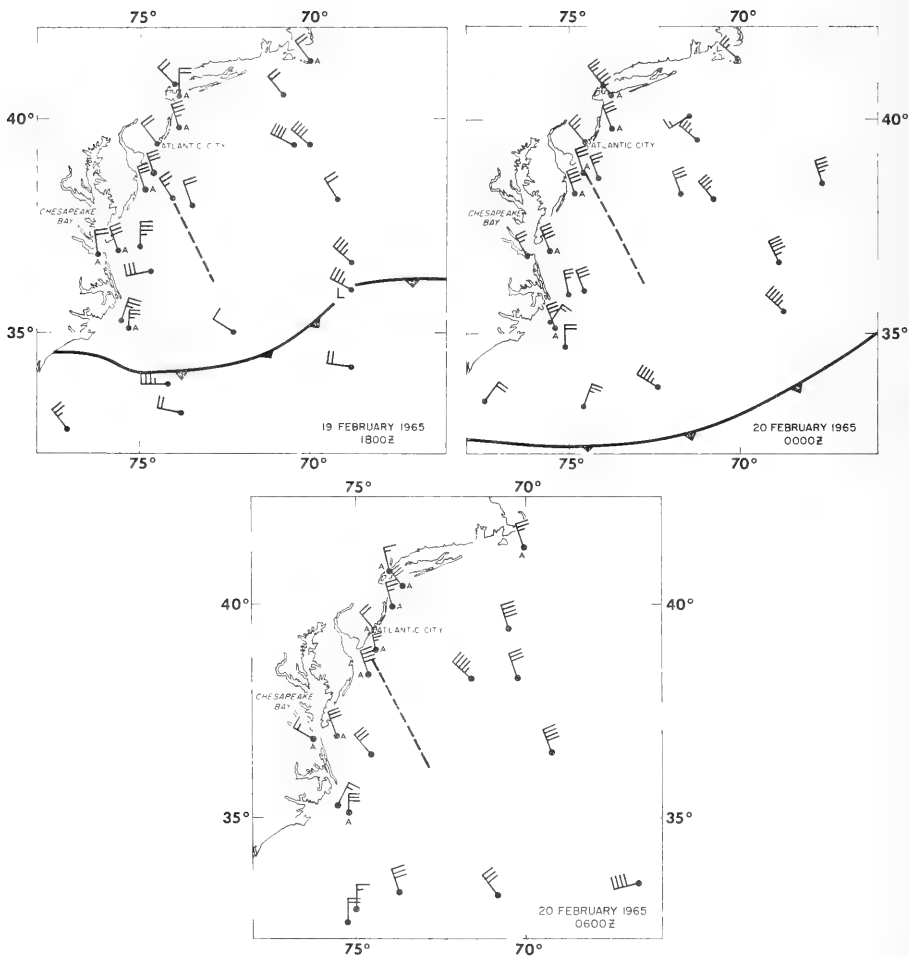
15

FIGURE 7.   a, b, and c. SEQUENTIAL WIND AND WEATHER MAPS
FOR COASTAL AND OFFSHORE AREAS OF THE MIDDLE
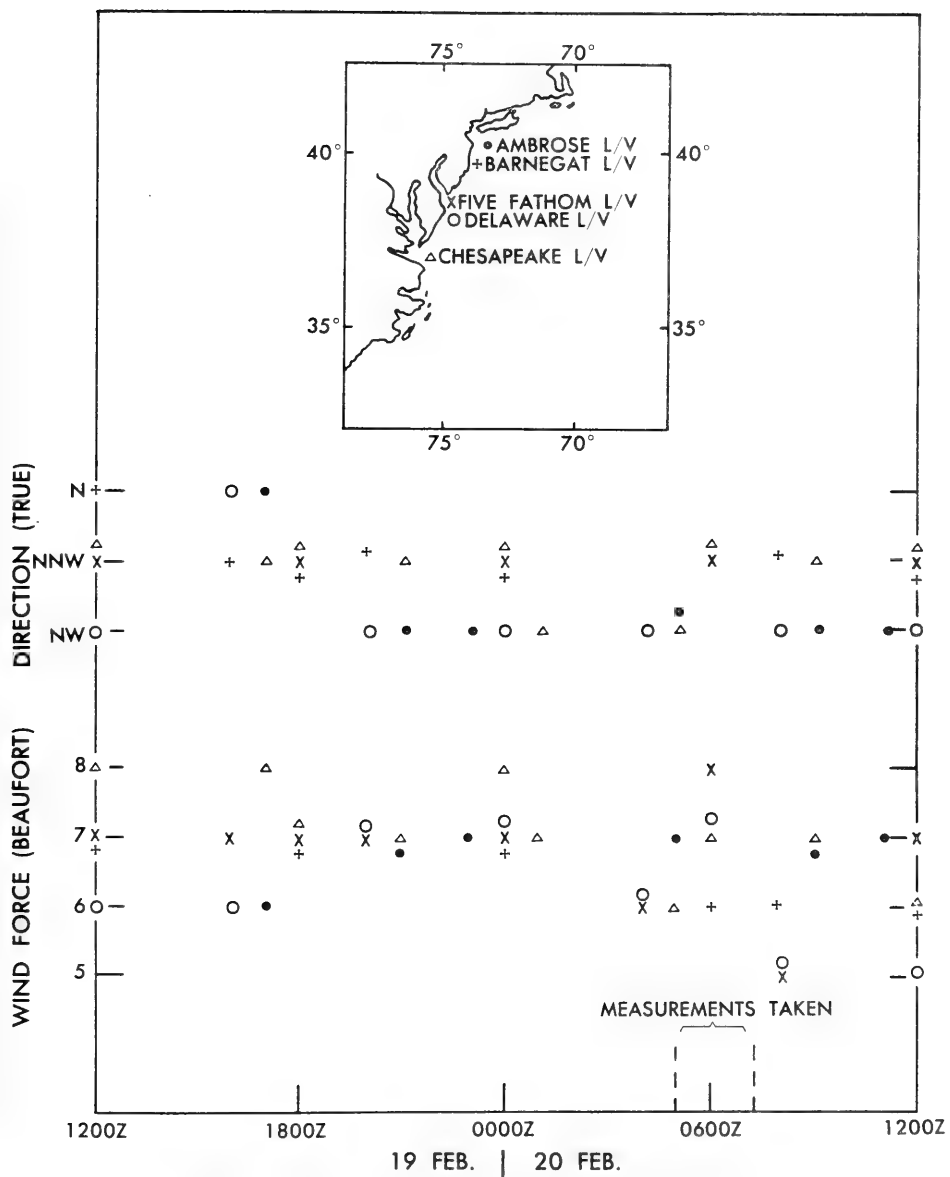ATLANTIC STATES, 1800Z, 2/19/65 to 0600Z, 2/20/65.

FIGURE 8. TIME HISTORIES OF WIND FORCE AND DIRECTION AT
OCEAN LIGHTSHIPS OFF THE MIDDLE ATLANTIC STATES.

was known by the power setting of the plane throttles, one simple subtraction yielded the effective wind speed. Due to the directions of the wind and of the plane flight, this effective wind speed was practically identical to the true wind speed at the altitude of the aircraft, 500 feet above the mean sea surface. The average wind on the downwind run was estimated by taking the total distance out from the coast that the plane travelled and dividing by the total time required to transverse this distance. The result was a 33 knot (17.0 m/sec) wind. Similarly, on the upwind leg the average wind was 30 knots (15.4 m/sec). It should be expected that these values will be a bit lower than the actual wind speed, since the plane did not fly a precisely straight line out from the coast.

To obtain an estimate of the uniformity of the wind field with distance from the coast, values of wind speed were calculated using successive five minute positions. The smoothed results are shown in Table 2. These data should be viewed with caution due to the relative inaccuracy of the smoothed LORAN A positions. The "downwind wind speeds" show a fairly large variability, but this was to be expected, since the plane's ground speed of approximately 220 knots will give rise to a larger positioning error. The "upwind wind speeds" are more uniform as the approximate ground speed here was 150 knots. Even after the problems and inaccuracies involved in plane positioning are realized, the results of Table 2 are unexpectedly good. This is due in no small part to the very careful and diligent efforts of the navigator and crew of the aircraft. A straight linear average shows a characteristic wind of 38.0 knots (19.5 m/sec) on the downwind leg and 34.7 knots (17.9 m/sec) on the upwind leg, both of which are somewhat higher than the total run estimates. Considering the altitude of the plane and the atmospheric stability, these wind estimates are in good accord with the lightship data. They further show that, at least in a relative way, the wind field was uniform with respect to distance from the coast. No attempt was made to reduce the plane winds to equivalent 10 meter winds.

The weather situation may be summarized by saying that the waves measured were generated by a steady, nearly offshore wind of speed 30-35 knots (15.4-18.0 m/sec) and direction 335°T which had been blowing for at least 12 hours but probably nearer to 16 hours. These were the large scale features of the wind field.

5.0   TREATMENT OF THE DATA

5.1   Spectral Analysis

Near continuous records of the sea surface profile from near the coast out to a distance of approximately 190 nm were obtained. Figure 2 is an example. Segments of the altimeter record taken within 50 nm of the coast were digitized at an interval of 0.05 second, while for all other parts of the record, the interval was

TABLE 2

WIND SPEED AS A FUNCTION OF DISTANCE FROM THE COAST
ESTIMATED FROM SMOOTHED, SEQUENTIAL LORAN A POSITIONS

DOWNWIND			UPWIND		
Distance (nm)	Wind (knots)	(m/sec)	Distance (nm)	Wind (Knots)	(m/sec)
25	40	20.6	18	34	17.5
52	37	19.0	33	34	17.5
78	42	21.6	52	35	18.0
98	37	19.0	70	34	17.5
115	33	17.0	98	30	15.4
135	33	17.0	115	34	17.5
155	44	22.6	135	30	15.4
180	38	19.5	145	36	18.5
			165	33	17.0
			185	47	24.2
Ave.	38.0	19.5	Ave.	34.7	17.9

0.01 second. If these time intervals seem quite small, it should be remembered that they are measured in the reference system of the rapidly moving airborne platform. In general, each resulting time (space) series consisted of 1200 or 1700 points depending on the direction of plane travel. Each series was numerically filtered prior to spectral analysis to remove extraneous low frequency noise. The apparent power spectra or spectra of encounter were computed on an IBM 7074 by the method of Blackman and Tukey (1958). These apparent spectra are designated by $E(\omega)$ where ω is the apparent frequency of encounter as seen by the plane. The apparent auto-correlation function is given as follows:

$$r(\tau) = \frac{1}{T} \int_{-T/2}^{+T/2} h(t)\, h(t + \tau)\, dt$$

with $h(t)$ being the time history of the sea surface as seen from the aircraft. The spectrum of encounter is:

$$E(\omega) = \frac{1}{\pi} \int_{0}^{\infty} r(\tau) \cos(\omega \tau)\, d\tau \,.$$

Each spectrum was independent of the other spectra in that any particular time series did not overlap those ahead or behind it. The raw spectra were corrected for instrument response and then smoothed using consecutive weighting factors of .23, .54, .23 (hamming). Due to the nature of the sea and the manner in which the measurements were made and digitized, "aliasing" did not introduce difficulties. The spectra of the data digitized at 0.05 sec were estimated over 100 lags. The corresponding 90 percent confidence limits are 0.65 and 1.39 for the downwind run, and for the upwind run, 0.71 and 1.32, respectively. The spectra of the data digitized at 0.10 sec have 90 percent confidence limits of 0.75 and 1.26 for downwind run and 0.76 and 1.24 for upwind run. While the confidence limits (degrees of freedom) for various runs and spectral estimates are not identical, they are not different enough to introduce statistical variability into the final results.

5.2   Numerical Filtering

A sample spectrum from the raw data is shown in Figure 9. The large amount of energy at low frequency precludes any meaningful statistical evaluation of the data. Such an evaluation must be made to determine the maximum length of record which can be considered as at least weakly homogeneous. The length of record used to produce Figure 9 corresponded to 6 nautical miles of sea surface at a distance of 150 nm from the coast. It will be shown that this interval is sufficient to ensure homogeneity.
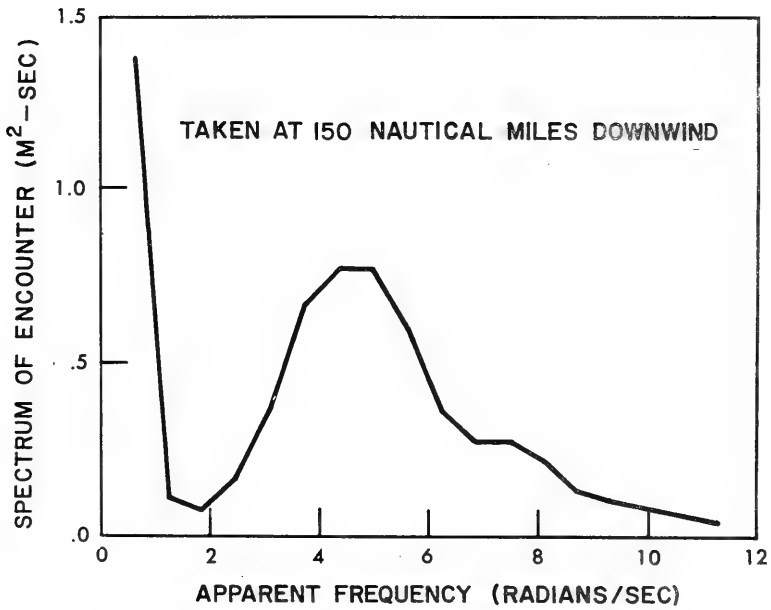
FIGURE 9. TYPICAL UNFILTERED SPECTRUM OF ENCOUNTER, E (ω).

The low frequency energy in Figure 9 is due to uncompensated plane motion. While the accelerometer cancels high frequency vertical plane motion, it cannot compensate for lower frequency components, nor can it account for rolling and pitching motions, all of which introduce ficticious wave energy to the apparent spectrum. It seems clear, based on Section 3.3, that these random motions of the aircraft do not materially affect the statistical character of the data in the frequency range that is here being described. This is further substantiated by the characteristic occurrence of the extremely deep "valley" in the spectrum near $\omega = 2$ rad/sec. Since the extraneous plane motion was due to random atmospheric turbulence, and because of the physical size of the plane, it seems most unlikely that the ficticious wave energy should rise again for $\omega > 2.0$ rad/sec. The low point of the valley is almost always within the noise level of the analysis.

In light of the preceding remarks, it was a relatively simple matter to construct a numerical filter that had the desired properties. The filter effectively discriminated only against disturbances with frequencies lower than 2.5 rad/sec, and therefore, the statistical character of phenomena with greater frequencies remained unaltered.

5.3   Statistical Tests

Once the data had been filtered, it was possible to apply various statistical tests in order to determine the most advantageous length of record for spectral analysis. The method was to break the entire record (extending from near the coast out almost 190 nm) into approximately one mile sections and then compare the statistics of a selected section with its neighbors. In this way it was possible to determine how many one mile sections could be considered as coming from the same population, and hence, the maximum permissible length of record that could be considered as being at least weakly homogeneous. Homogeneity thus means that the average properties of each of the segments of sea surface, making up the length of record to be analyzed, must be practically the same. The reader is reminded that the conditions for stationarity have been obtained in Section 2.0.

By the very nature of the filtering process, the mean of each section of data was set to zero. The 2nd, 3rd, and 4th moments about the mean were left to provide the needed information. No tests could be found that allowed comparisons of 3rd and 4th moments, and so it was not possible to determine "complete" homogeneity limits. With the second moment, variance, however, it was possible to set upper bounds for the condition of "weak homogeneity". In this respect, the 3rd and 4th moments were useful in the sense of providing consistency to the analysis.

Two methods of comparing variances were used: Cochran's Test and Bartlett's

Test.* The first test compares the maximum variance to the sum of all of the neighboring variances, while the second allows a more complicated comparison through an F—test. A significance level of .05 was used in both cases. It turned out that in the inner region (0–50 nautical miles from the coast) a stretch of sea surface approximately 3 miles long could be considered as weakly homogeneous. For the outer region (distances greater than 50 nautical miles) this length increased to approximately 7 miles. Obviously, the transition from the 3 to 7 mile length was not abrupt. By considering it as such, we give up some spectral confidence in the 35–50 mile range, but this is made up for by the gain in uniformity of analysis.

6.0   THE SPECTRAL TRANSFORMATION

6.1   The Frequency Transformation

The problem of relating the frequency and direction of a free wave to its apparent frequency and direction, as observed from a moving platform, has been discussed in detail by St. Denis and Pierson (1953) and also by Snyder and Cox (1966). The practical aspects of the frequency mapping and spectral transformation have been put forth by Cartwright (1963). Cartwrights paper was of considerable assistance in the mathematical formulation of this section.

The relation between real wave frequency σ and the apparent wave frequency ω is

$$\omega = \sigma - \frac{\sigma^2 V \cos \psi}{g}, \tag{5}$$

where V is the speed of the moving platform and ψ is the angle between the direction of platform motion and the direction of wave propagation. The basic equation (5) will give a unique value of ω for any fixed values of σ and ψ. On the other hand, the inverse relation

$$\sigma = \frac{1 \pm \sqrt{1 - (4\omega V \cos \psi)/g}}{2 V \cos \psi /g} \tag{6}$$

is non–unique. The speed of the platform and the value of ψ determine which branch of (6) is to be considered. Cartwright gives a very succinct discussion of the various possibilities of this determination, therefore, such a summary will not be repeated here. It will suffice it to say, the problem is a bit complicated for the general situation in which the speed of the platform can be less than the speed of the fastest wave. In this case,

*The generous assistance of Dr. H. C. S. Thom in making these choices is gratefully acknowledged.

however, the plane was going much faster than the fastest wave being observed. Furthermore, the plane was "seeing", what was for all practical purposes, a pure wind sea. Thus, it is most reasonable to assume that nearly all of the wave energy was confined within ±90° of the mean wind direction. These facts indicate that the plane will always be overtaking the waves as it moves in the downwind direction. From (5), ω will be negative and it is convenient to redefine ω and σ as

$$\omega = -\sigma + \frac{V\sigma^2}{g}\cos\psi \qquad\qquad |\psi| < \frac{\pi}{2} \qquad\qquad (5a)$$

$$\sigma = 1 + \frac{\sqrt{1 + \dfrac{4V\omega}{g}\cos\psi}}{\dfrac{2V}{g}\cos\psi} \qquad\qquad |\psi| < \frac{\pi}{2} \qquad\qquad (6a)$$

This corresponds to the case of the plane travelling downwind. A similar re-definition of ω and σ may be made for the case where the plane is travelling upwind. These definitions are made merely to maintain consistency in the analysis of any particular run.

6.2   Specifications of the Integral Transform

        The relation between the apparent spectrum $E(\omega)$ and the real two-dimensional spectrum, relative to the plane heading $F(\sigma,\psi)$, may be expressed in either of two forms:

$$E(\omega) = \int_{c_1} F(\sigma,\psi) \left| \frac{\partial\psi}{\partial\omega} \right| d\sigma \qquad\qquad (7)$$

or

$$E(\omega) = \int_{c_1} F(\sigma,\psi) \left| \frac{\partial\sigma}{\partial\omega} \right| d\psi \qquad\qquad (8)$$

where c_1 indicates that the integration is to be carried out over all σ and ψ which can yield the specified value of ω (Cartwright, 1963). In the case of the plane travelling downwind, σ and ψ together must satisfy equation (5a) and (6a) with ω fixed. The corresponding Jacobian's would be

24

$$\frac{\partial \psi}{\partial \omega} = \left(\frac{V\sigma^2 \sin\psi}{g}\right)^{-1}, \text{ with } \cos\psi = \frac{(\sigma + \omega)\,g}{\sigma^2 V},$$

and $\quad \dfrac{\partial \sigma}{\partial \omega} = \left(1 + \dfrac{4\,\omega V}{g} \cos\psi\right)^{-1/2},$

with σ from (6a).

To obtain a solution of (7) and (8) it was necessary to represent the two dimensional spectrum as a product of a frequency-dependent function and an angular spreading factor,

$$F(\sigma, \psi) = H(\sigma)\, K(\sigma, \psi).$$

In this experiment the plane tracks were only upwind or downwind, and therefore, it was not possible to obtain direct estimates of $K(\sigma, \psi)$. Hence, it was necessary to make various assumptions concerning this function and then see how sensitive the results were to these assumptions. Three forms of K were considered:

(i) $\quad K(\sigma, \psi) = K_1(\psi) = \delta(\psi),$

(ii) $\quad K(\sigma, \psi) = K_2(\psi) = \dfrac{8}{3\pi} \cos^4\psi \qquad\qquad |\psi| < \dfrac{\pi}{2}$

$\qquad\qquad\qquad\qquad = 0, \qquad\qquad\qquad\qquad |\psi| \geq \dfrac{\pi}{2}$

(iii) $\quad K(\sigma, \psi) = K_3(\sigma, \psi) = g(\sigma)(\cos\psi)^{p(\sigma)} \qquad |\psi| < \dfrac{\pi}{2}$

$\qquad\qquad\qquad\qquad = 0. \qquad\qquad\qquad\qquad |\psi| \geq \dfrac{\pi}{2}$

Each of the K's has been centered on the plane's heading which, since it was essentially downwind, is considered as relative zero. K_1 is a delta-function and is equivalent to assuming that all of the waves were travelling directly downwind. K_2 gives an angular spread that is independent of frequency and is normalized so that

$$\int_{-\pi/2}^{+\pi/2} K_2(\psi)\, d\psi = 1.$$

The actual directional properties of the spectrum seem to lie somewhere in between these two forms. Hence, a third spreading factor was constructed that had the

25

essential directional properties found by both Longuet-Higgins, et al., (1963) and SWOP I (Cote, et. al., 1960): Waves moving at nearly the speed of the wind $(W/c - 1)$ were concentrated in a rather narrow angular beam about the wind direction $(\psi = 0)$. The width of this beam increases as the ratio W/c increases. In the definition of K_3, then, the exponent $p(\sigma)$ will be large for $W/c \sim 1$ and diminish as W/c becomes large relative to 1. The function $p(\sigma)$ is shown versus W/c in Figure 10 and compares well to the results of Longuet-Higgins, et. al.,(1963) as amended by Cartwright (personal communication). The normalizing factor $g(\sigma)$ is chosen so that

$$\int_{-\pi/2}^{+\pi/2} K_3(\sigma, \psi) \, d\psi = 1$$

and therefore

$$g^{-1}(\sigma) = \int_{-\pi/2}^{+\pi/2} \cos^{p(\sigma)} \psi \, d\psi \; .$$

In order to estimate the effect of different directional assumptions, the integral equations (7) and (8) were solved for all three of the K's. It should be noted that in carrying through these solutions, the assumption has been made that each K is independent of fetch.

6.3   Solution of the Integral Equations

This section proceeds to outline the solution of equations (7) and (8). Although the present discussion concerns only the case of the plane travelling downwind, it should be clear that it applies equally well to the upwind case, provided ω, ψ, and $K(\sigma, \psi)$ are defined properly.

Substituting for $F(\sigma, \psi)$ and the Jacobians, one has

$$E(\omega) = \int_{c_1} \frac{H(\sigma) \left[K(\sigma, \psi) + K(\sigma, -\psi) \right] \, d\sigma}{\frac{\sigma^2 V}{g} \sin |\psi|} \tag{7a}$$

and

$$E(\omega) = \int_{c_1} \frac{H(\sigma) \left[K(\sigma, \psi) + K(\sigma, -\psi) \right] \, d\psi}{\sqrt{\frac{1 + 4\omega V \cos \psi}{g}}} \; . \tag{8a}$$

26
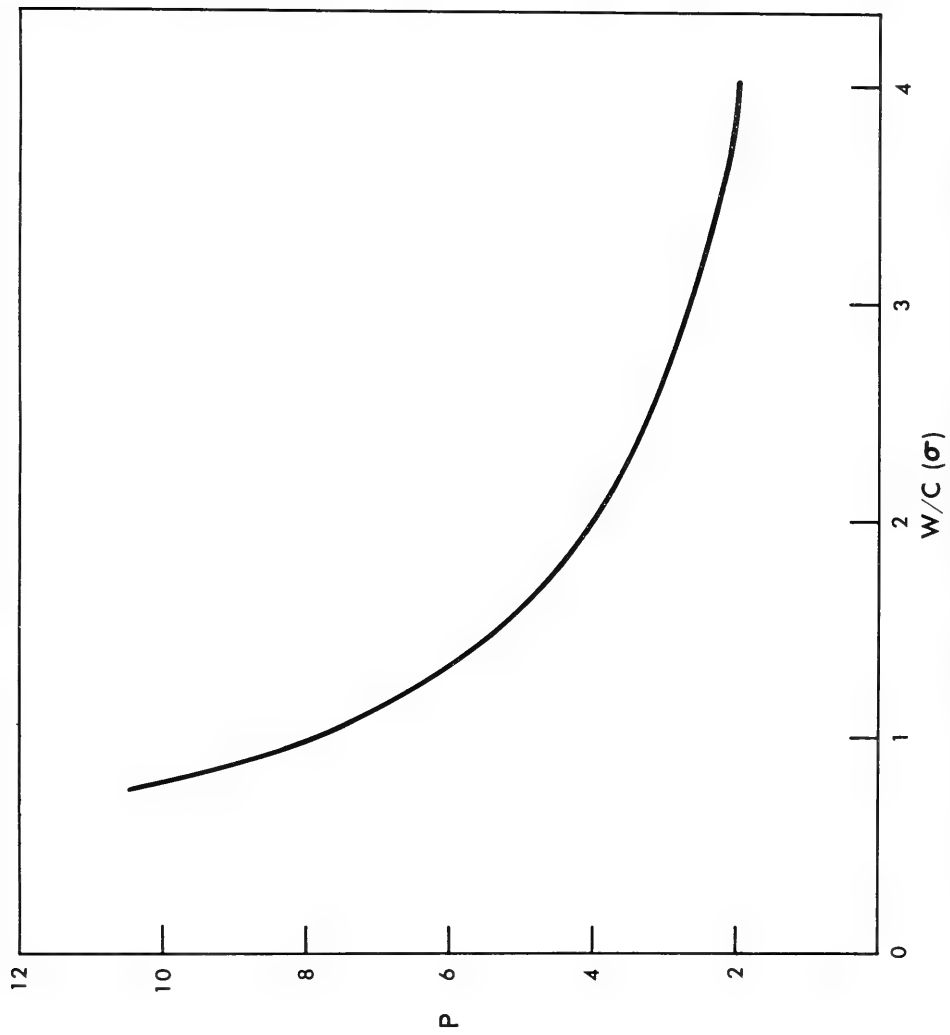
FIGURE 10. EXPONENT OF SPECTRAL DIRECTIONALITY, p, VERSUS W/c (σ) FOR THE K_3 ASSUMPTION.

These equations will be recognized as similar to Fredholm integral equations of the first kind since $\psi = \psi(\sigma, \omega)$. As if this were not bad enough, the kernel function, while symmetric with respect to direction (i.e., $K(\sigma, \psi) = K(\sigma, -\psi)$, is not symmetric in the more general sense of $K(\sigma, \psi) = K(\psi, \sigma)$. The theory of this type of equation is not well developed. It may be surmised though, that even if the non-symmetric kernel does possess real, non-zero eigenvalues, the best that can realistically be hoped for in a solution to the equation is a type of mean value for $H(\sigma)$ in a specified σ - interval. This seems perfectly alright, however, since $E(\omega)$ is only an estimate in a similar frequency interval in ω — space. The solution then will represent a smoothed approximation to the exact answer.

The problem of solving (7a) or (8a) can be considered as a generalization of the problem of solving a set of n-algebraic equations in n-unknowns. With this idea in mind (7a) may be approximated as follows:

$$E(\omega_i) = \int_{c_1} \frac{H(\sigma)\left[K(\sigma, \psi) + K(\sigma, -\psi)\right]d\sigma}{\frac{\sigma^2 V}{g}\left|\sin\psi\right|} \tag{9}$$

$$=\sum_{j=1}^{n} \frac{H(\sigma_j)\left[K(\sigma_j, \psi_{ij}) + K(\sigma_j, -\psi_{ij})\right]\delta\sigma_j}{\frac{\sigma_j^2 V}{g}\left|\sin\psi_{ij}\right|}$$

$$=\sum_{j=1}^{n} A_{ij} H(\sigma_j).$$

Note that the finite difference representation is general enough to allow for unequal intervals of σ_j. In this notation, σ_j and ω_i represent individual members of a discrete set of mid-interval frequencies, while ψ_{ij} is the value of ψ determined by

$$\psi_{ij} = \cos^{-1}\left[\frac{(\sigma_j + \omega_i)}{\sigma_j^2 V}\, g\right].$$

The idea is to fix upon values of ω_i and σ_j, and with ψ_{ij} from above, evaluate the coefficients A_{ij}. For the values of σ_j and ω_i for which $\psi - \delta\psi < 0 < \psi + \delta\psi$, A_{ij} must be evaluated from (8a) due to the singular nature of (7a) at $\psi = 0$. In this case $H(\sigma)$ varies but slightly over the interval ψ equals 0 to $\delta\psi$ and so may be considered as constant in that range (Cartwright, 1963). Hence, (8a) is approximated

by

$$E(\omega_i) = \frac{H(\sigma')}{\left[1 + \frac{4\,\omega_i\,V}{g}\right]^{1/2}} \int_0^{\delta\psi} \left[K(\sigma',\psi) + K(\sigma',-\psi)\right]\,d\psi \qquad (10)$$

where σ' is the given value of σ_j from the discrete σ-set for which ψ_{ii} at ω_i is nearest to zero. The desired value of A_{ij} may be readily calculated.[i] Values of σ_j less than σ' cannot give a contribution to E at the particular ω_i, and hence the corresponding coefficients of A-matrix must be zero. The single integral equation is finally reduced to a set of n-linear algebraic equations in n-unknowns.

$$\left[E(\omega_i) - \sum_{j=1}^{n} A_{ij}\,H(\sigma_j) = 0\right] \qquad i = 1, n \qquad (11)$$

The E's are given and the terms of the coefficient matrix A_{ij} have been determined in the most appropriate manner.

It is now left to solve these equations for the desired unknowns, $H(\sigma_j)$. Affecting this solution is not the easy matter that it would appear, for merely reducing a Fredholm equation of the first kind to a set of linear algebraic equations is not a magic vehicle to simple solution of the original equation. The biggest problem that arises is that the set of algebraic equations may be "ill-conditioned", which is another way of saying that various of the equations may be dependent or nearly so. A simple test for ill-conditioning is given by Redish (1961). Geometrically stated, the test is as follows: Each equation of set (11) may be thought to represent a hyper-plane. If two or more of these hyper-planes are nearly parallel, the set is said to be illconditioned. To calculate the actual angle between the hyperplanes, the equations are first normalized by dividing each equation by the square root of the sum of the square of its coefficients. The new coefficients, A'_{ij} say, are now the direction cosines of the normals of the hyper-planes. The angle ⒣$_{lm}$ between the lth and m^{th} hyper-planes can be calculated since

$$⒣_{lm} = \cos^{-1} \left(\sum_{j=1}^{n} A'_{lj}\,A'_{mj}\right)$$

The nearer the angle ⒣$_{lm}$ is to zero, the more poorly conditioned (dependent) are the lth and m^{th} equations.

To suitably condition the equations (11) (i.e., to maximize ⒣$_{lm}$) it is necessary to choose the values σ_j in a judicious manner. This is necessitated because of the complicated relation between σ and ω and because some σ-values will not be able

to contribute to the whole range of ω. Hence, to avoid developing quasi-dependent or redundant equation pairs, it is necessary to pick the σ_i in such a way that no one σ -interval will contribute the <u>majority</u> of the energy in two successive ω -intervals.

The equations that finally result from a triangular array of dimension 30 and, because of the finite difference approximation, represent the original integral equation plus a slight perturbation term ϵ (ω). The corresponding form of (7a) would be

$$E\ (\omega)\ +\ \epsilon\ (\omega)\ =\ \int_{c_1}\ F\ (\sigma,\psi)\ \left|\frac{\partial\psi}{\partial\omega}\right|\ d\sigma \tag{12}$$

A measure of the degree of accuracy of the approximation, and hence ϵ (ω), was obtained in the following way. A known H (σ) was supplied to (7a) and (8a) and E (ω) directly evaluated to four decimal places by Simpson's rule integration. Using this E (ω), the equations

$$\mathbb{A}\mathbb{H}' \equiv \mathbb{E}$$

were solved for H' on an IBM 7094 computer. The ratio H' (σ)/ H (σ) then gives the required accuracy measure as a function of frequency.

The input H (σ) that was used was the latest Pierson-Moskowitz (1963) empirical wave spectrum,

$$H\ (\sigma) = \frac{d_1 g^2}{\sigma^5}\ \exp\ \left[-d_2\left(\frac{g}{\sigma\ W}\right)^4\right]$$

where $d_1 = 8.1 \times 10^{-3}$ and $d_2 = 0.74$. The directionality is assumed proportional to $\cos^4$ and normalized as before (K$_2$). For the comparison, wind speeds of 18 and 30 knots (9.3 and 15.4 m/sec) were used. The given H (σ), estimated H' (σ) and ratio of H'/ H are shown in Figure (11).

For the 18 knot test case, the agreement between H and H' is quite good with an error of about 1.5% near the spectral peak. For the 30 knot case, the error is approximately 3% near the peak but almost 10% for the last (lowest) value of σ. This is due to a combination of rapid changes of H and the grossness of the finite difference approximation to the original integral in the low frequency range. Although an error of 10% is acceptable, in practice no significant energy will be found at these lowest frequencies, and so the accuracy is somewhat better than 10%.

It should be mentioned in passing that since there is an upper limit (σ_{max}) on the σ -range that is being considered, it should be necessary to subtract from all of the E (ω), the contribution due to $\sigma > \sigma_{max}$. This would be done by evaluating the integral via Simpson's rule, as before, from σ_{max} to σ equal, say 4π. Waves with frequencies greater than 4π contribute essentially nothing to the frequency range
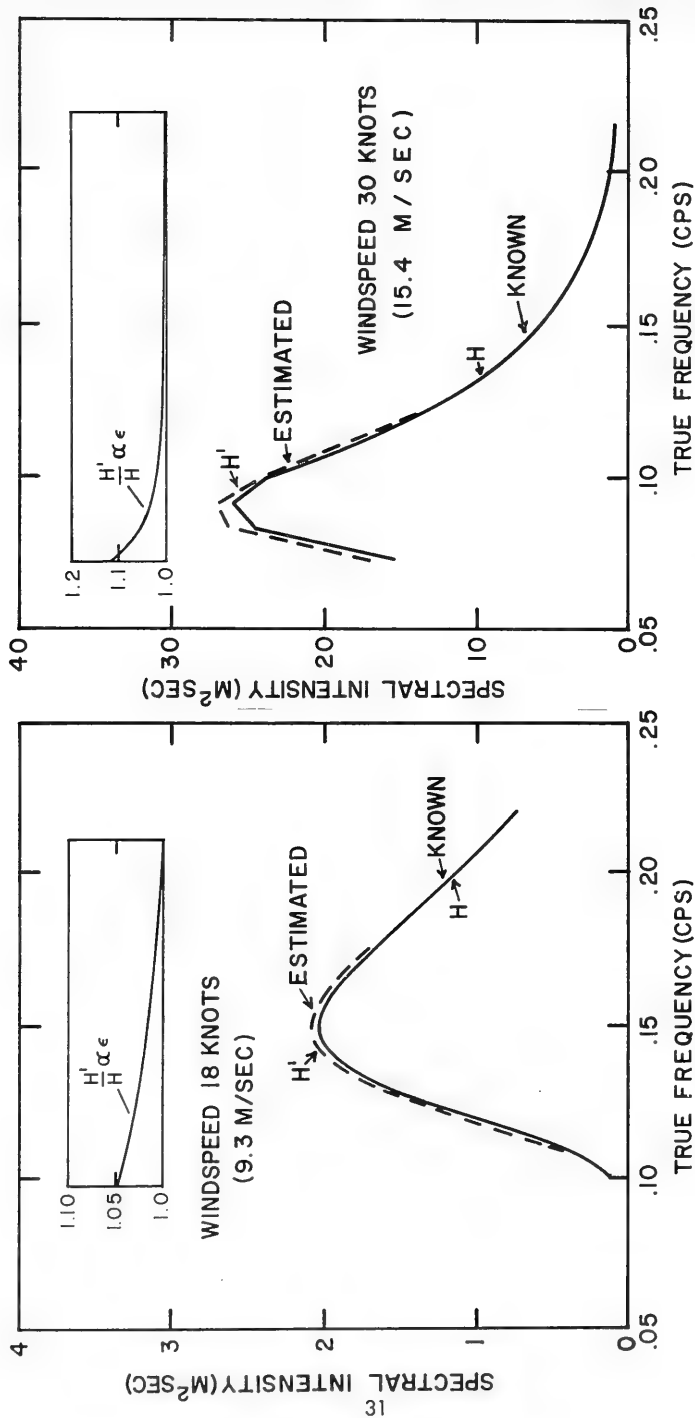
FIGURE 11. KNOWN AND ESTIMATED SOLUTIONS TO THE INTEGRAL EQUATION FOR TWO TYPICAL PIERSON-MOSKOWITZ EMPIRICAL SPECTRA.

31

presently being considered. Such corrections were indeed made to obtain the results of Figure 11. In practice, the function $H(\sigma)$ in this region would be approximated reasonably well by

$$H(\sigma) = d_3 g^2 \sigma^{-5} \qquad . \qquad (13)$$

This is the equilibrium spectrum proposed by Phillips (1958b), with d_3 equal to an empirically determined, universal constant. However, the amount of noise present in the experimental $E(\omega)$'s is an order of magnitude greater than the correction term under discussion. There is enough uncertainty in this noise level so that, in general practice, it was not realistic to attempt this relatively fine scale correction. This, of course, implies, and rightfully so, that the estimates that will be made of the high frequency portion of the spectrum are not particularly accurate. This should come as no great surprise, however, since the very nature of the instrument response (Section 2.3, Figure 4) indicates that reasonably exact estimates of high frequency spectral components are not possible with the airborne sea-swell recorder.

6.4   Definition of the Spectral Field

In presenting the final estimates of spectral energy at various distances from the coast, it has been convenient to speak in terms of true frequency, $f = \sigma/2\pi$, and the true frequency spectrum, $F(f, \psi, x) = 2\pi F(\sigma, \psi, x)$. Figures 12 and 13 show contours of the quantity $F(f, o, x)$ for the various directional assumptions and plane headings. This is similar to the type of presentation that has often been used by Munk and his co-workers in tracking swells from distance storms (e.g., Munk, et.al., 1963). Henceforth, all references to the spectrum will be directed toward the quantity $F(f, o, x)$.

The contours on each f-x diagram are based on approximately 22 values of F vs f for each of 27-30 different x's ($\sim$ 600 points/diagram). The x-axis is directed downwind and x equals zero at the coast line. The grid spacing along the x-axis was 3.5 nautical miles for the inner region and 7.0 nautical miles for the outer region. Along the f-axis the grid spacing decreased from .011 cps near $f \approx .08$ cps to .004 cps at $f \approx .20$ cps. The philosophy used in contouring was to show as much detail as possible with a minimum of smoothing. In this way it was felt that the data would be presented as objectively as possible. As luck would have it, no data were obtained for the region between about 15 and 25 nautical miles from the coast. This made it impossible to discuss the growth of the higher frequency waves.

In viewing the f-x diagrams there are several important items to bear in mind. A cut along the f-axis at constant x will give the spectrum F(f,o) at x. Similarly, a cut along the x-axis at constant f will give the spatial history of the f-spectral

32
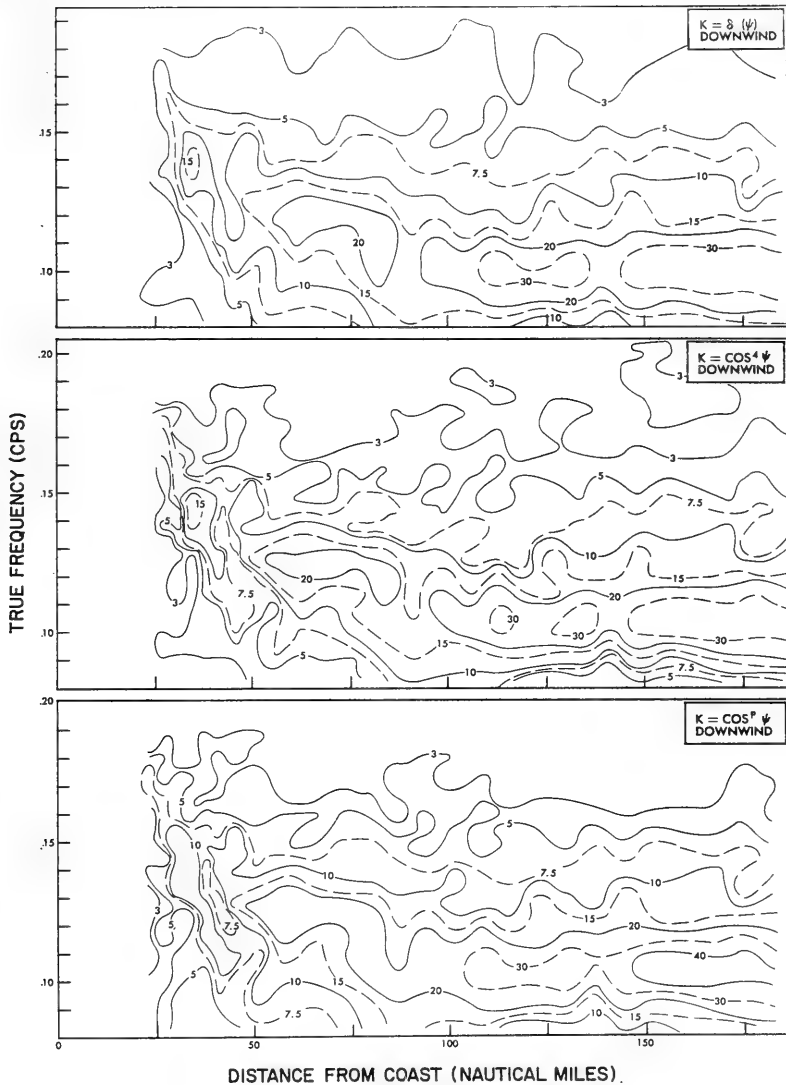
FIGURE 12. CONTOURS OF EQUAL SPECTRAL DENSITY (m^2 - sec) ON A FREQUENCY-DISTANCE PLOT FOR THE DOWNWIND RUN AND VARIOUS DIRECTIONAL ASSUMPTIONS.
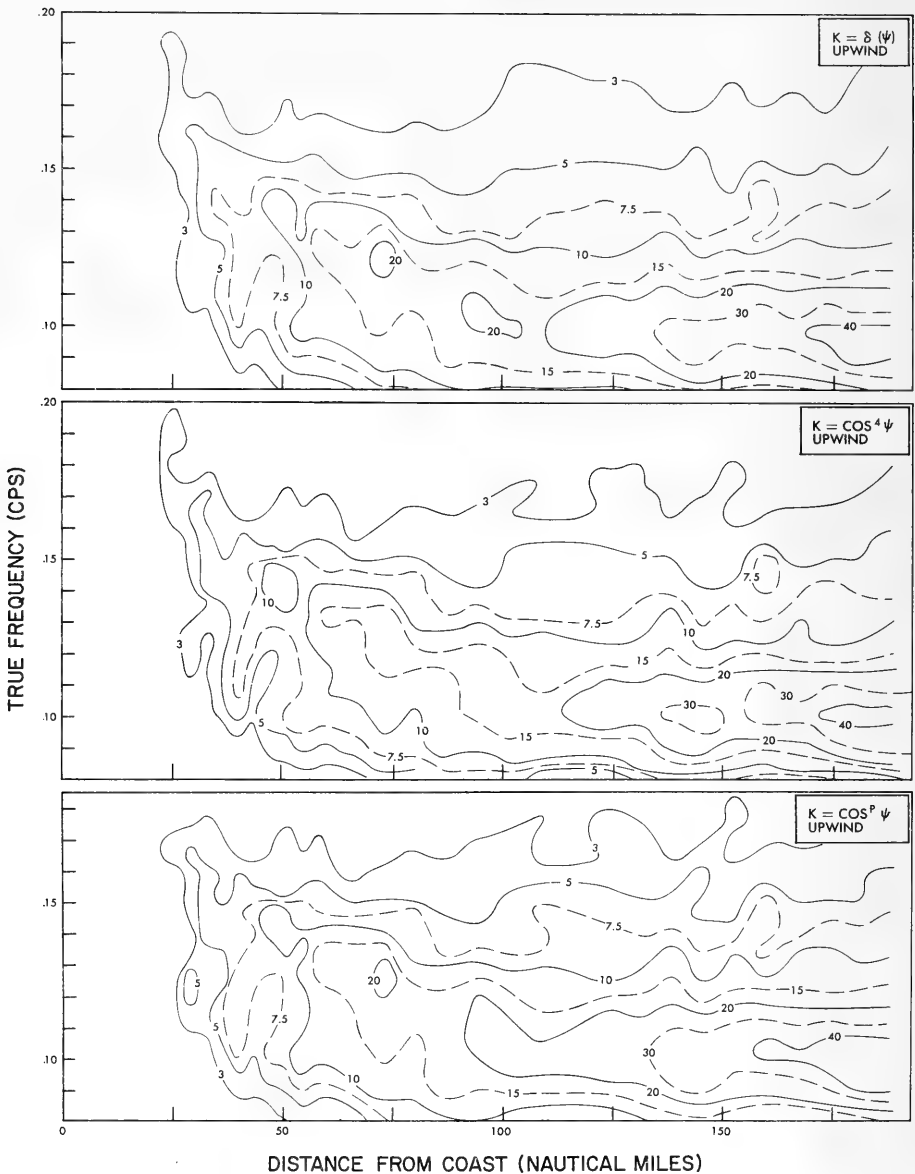
FIGURE 13. CONTOURS OF EQUAL SPECTRAL DENSITY (m^2 - sec) ON A FREQUENCY-DISTANCE PLOT FOR THE UPWIND RUN AND VARIOUS DIRECTIONAL ASSUMPTIONS.

component. Also of interest are the location of spectral peak(s) or valley(s) at any particular x-value and the value of x beyond which a specified spectral component may be considered to be in equilibrium. In the first case $\partial F / \partial f = 0$ and the tangent to a particular F-contour will be parallel to the f-axis. On the other hand, for an equilibrium condition $\partial F / \partial x = 0$ and the contour tangent will be parallel to the x-axis.

7.0   RESULTS

7.1   Qualitative Discussion of the f-x Diagrams

It is apparent from Figures 12 and 13 that the type of spreading factor used to solve (7a) and (8a) had little qualitative effect on the outcome of the results. This is due to the fact that while each of the spreading functions used had a different mathematical form and physical interpretation, they all confined the wave energy to a fairly narrow, directional band about the wind direction. An isotropic spreading factor, say, would have yielded quite different and quite unrealistic results.

Another general comment that can be made is that the upwind diagrams appear to have somewhat less energy content than the downwind diagrams. To some extent this is true, but the effect is exaggerated by two facts. The area of greatest apparent difference is generally in f-x regions where $\partial F / \partial x$ is relatively small. Hence, small changes in F significantly affect the position of a contour line. This, coupled with the contouring philosophy, partially accounts for the apparent result. However, it is obvious that the f-x structure of the inner region is somewhat different between the downwind and upwind runs. The discussion of this feature is deferred for the moment.

The essential features of the diagrams are:

(i)   The major spectral peak migrates toward lower frequencies with increasing distance from shore. This feature, which was no surprise, is further illustrated by showing the frequency of the major spectral peak, f_o, versus x (Figure 14). The shape of this curve is similar to that found by Hidy (1965) in wave channel experiments. The form of the curve strongly hints at the importance of an instability-type of wave generation mechanism.

(ii)   There is a considerable amount of wave energy in the low frequency end of the spectrum for even the small values of x. This indicates that energy was being simultaneously added over the whole frequency range of the spectrum. This result is in conflict with the concept that a given frequency component must be almost "fully developed" before a lower frequency component can begin to grow, (e.g., Pierson, et. al., 1955, Baer, 1962).
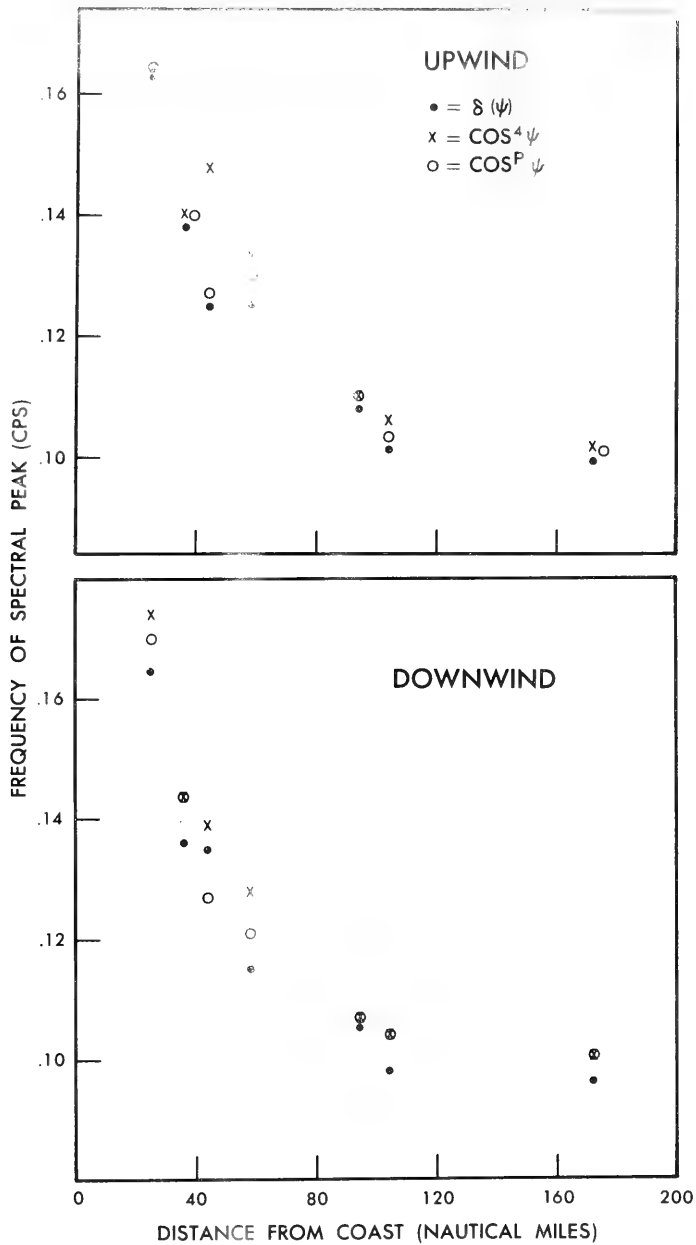
FIGURE 14. FREQUENCY OF THE SPECTRAL PEAK AS A FUNCTION OF DISTANCE FROM THE COAST.

It is interesting to note that there is some tendency for a secondary spectral peak to appear near the approximate wind frequency f_W ($f_W = g/2\pi W \approx$ 0.10 cps). This is the frequency at which the Phillips' mechanism would be expected to be most effective in generating waves. However, this apparent feature of the f-x diagrams is only mentioned in passing and cannot be taken seriously on the basis of the present data. All that can be said is that there was a significant amount of energy spread over the entire low frequency range and that all frequencies appear to be growing simultaneously.

(iii) Consider a cut along the x-axis for fixed frequency f' somewhat greater than f_W. The magnitude of the f' component will increase with x until at some distance $x = x_m$, f' will be the location of the spectral peak and $F(f', x_m) = F_m$. It would traditionally be expected that for all $x \geq x_m$, $F \approx F_m$. The f-x diagrams indicate that this is not the case. Instead, for $x > x_m$, it will be observed that F is always less than F_m and by a statistically significant amount. In physical terms this means that as a spectral component grows, it apparently "overshoots" its eventual equilibrium value. Thereafter, the component gives up energy and soon settles down to the final equilibrium value. For the highest frequencies shown on the diagrams this effect is obscured by the fact that the area in which the overshoot occurs was not sampled. A more quantitative discussion of the entire phenomena is given in Section 7.3.

To attempt to explain completely the "overshoot" behavior of the individual spectral components is beyond the scope of this paper. One might speculate, however, that the phenomena is the result of some wave breaking, wave-wave interaction type of effect. Alternatively, one might imagine as did Neumann and Pierson (1963) that the occurrence of breaking seas of approximate frequency f' tends to cause partial annihilation of wave energy associated with frequencies $f \geq f'$. Waves with frequencies less than f' would feel little or no effect of this breaking since their wave lengths are greater than the scale of wave induced turbulence. All of this suggests that the actual representation for the one dimensional equilibrium spectrum (Equation 13) might be closer to that considered briefly by Phillips (1963),

$$H(f) \propto g^2 f^{-5} \cdot R(f_o/f) \qquad (14)$$

where R is a dimensionless function of f and the frequency of the local spectral peak is f_o. The true frequency has been used in place of circular frequency in order to maintain consistency in the discussion. The form of Equation (14) raises some rather fundamental questions concerning the causes of the equilibrium range. Implicit in Phillips' (1958B) formulation of the equilibrium theory was the assumption that wave breaking was local "at a point". However, localness in $\overrightarrow{x}$-space does not necessarily imply localness in f-space and, therefore, a simple form such as Equation (13) need not adequately describe the equilibrium range. In fact, Equation (13) was only meant

37

to give an upper limit to the magnitude that any particular spectral component could attain. This does not imply that this upper limit is ever reached or, if reached, maintained.

(iv) Attention is now returned to the features present in the near zone of the f-x diagrams. The most obvious of these is the occurrence of a "peak" (high wave energy) and then a "valley" (low wave energy) in the downwind diagrams in the region $f = .12 - .15$ cps and $x = 35 - 45$ nautical miles. These features do not repeat in the upwind diagram, but considerable certainty can be attached to the belief that the features are indeed real. This raises the problem of trying to explain their cause. Since the frequencies involved indicate that the corresponding waves are in relatively deep water, there is little possibility of accounting for the result through shoaling or some other bottom effect. The only other explanation that seems at all reasonable was the presence of a small area of relatively stronger wind located some 35 nautical miles from the coast. Since the plane was travelling much faster than this area, the result would be shown on the f-x diagrams as an area of high wave energy. Frequencies higher than those in the peak area would already be at or near equilibrium and hence shown no significant change. Frequencies lower than the peak respond more slowly to changes in wind speed and once again show little evidence of such an area. If one takes this point of view, the "valley" is now only a relative feature due entirely to the occurrence of the peak area. A close inspection of the upwind and downwind diagrams will show that the energy content of the valley area (in f-x space) is practically the same for both. While the occurrence of an area of stronger wind accounts qualitatively for the observations, and at the same time does not strain one's imagination, such an explanation must be considered as speculation. There are no definite facts to back it up. This indicates how vital it is to know more about the fine scale features of the wind field. At the same time it points up the folly of attempting anything but a macroscopic analysis of the present, limited data.

One other near zone feature of the f-x diagrams deserves comment. This is the presence of a shallow, upward sloping valley in the region (.09, 45). The fact that this feature appears on both sets of diagrams and at essentially the same location indicates that it is significant. Detailed topographic charts show that the flight path of the aircraft crossed over a north-south extending ridge on the sea floor at a distance of 42 nautical miles from the coast. The ridge was just shoal enough to make waves with frequencies less than 0.10 cps feel bottom. Although this undersea ridge could account for the above mentioned f-x feature, the magnitude of the effect is small in comparison with the statistical variability inherent in the spectral estimates. The error will be presently neglected, but hopefully not repeated in later work.

7.2   Wave Growth

7.2.1   Determination of Wave Growth Parameters

It is the purpose of this section to obtain quantitative estimates of the wave growth parameters α and β (Equation 2), and then to compare these estimates with

theory. Before proceeding it was necessary to retrieve spectral growth data from the f-x diagrams. This was simply done by taking cuts along the x-axis for various frequencies. A selected amount of this growth data is shown in Appendix A. Also shown are the best fit growth curves obtained in this section.

Since the theory of Section 2.0 concerns itself with only the linear phases of wave growth, it was necessary to use only data for which nonlinear effects were small. A good rule of thumb is that nonlinearities are negligible as long as the magnitude of a particular spectral component is less than 30% of its maximum value (Snyder and Cox, 1966). Further limitations are imposed by the fact that no data were obtained for the area between 15-25 nautical miles from the coast and also that data from the downwind near zone "peak area" was useless. With these restrictions only a small amount of the growth data was available for analysis. Once this data had been isolated, α and β were evaluated by the method of least squares so that the quantity

$$\sum w_i \left[F(x_i) - S(x_i, \alpha, \beta) \right]^2$$

was a minimum. $F(x_i)$ is the observed value of a spectral component at the position $x = x_i$, S is the estimated value of F at x_i, and w_i are weighting factors. The w_i are chosen so as to be inversely proportional to the square of $F(x_i)$ unless $F(x_i)$ is less than $1m^2$ - sec in which case $w_i = 1/F(x_i)$. Such a system tends to give equal weight to each data point but discriminates against values below $1m^2$ - sec where noise is more important. A comparable weighting scheme was employed by Snyder & Cos. The resulting best estimates of α and β are shown versus wave frequency for the various spreading factors in Figures 15 and 16, respectively. Also shown on these figures are the theoretically predicted α and β as discussed in the following sections. No effort will presently be made to estimate the directional aspects of α and β.

7.2.2 Linear Wave Growth

The results of the previous section indicate that the linear growth factor, α, is important in the initial generation of wind waves and in providing a substantial amount of the energy near the eventual spectral peak. However, the magnitude of α is sufficiently small so that it cannot account for a majority of the observed wave energy at the more advanced stages of spectral development. Also, apparent from Figure 15 is that the choice of directional assumption had little significant influence on the estimates of α for an individual run. To be sure, there was almost a factor of two difference in the corresponding magnitudes of the estimates, but in view of what is to immediately follow, this is of small concern. The important thing is that the dependence of α on frequency is clearly the same for all three K's.

The relative magnitude and distribution of α with frequency appear somewhat different between the two runs. The maximum value of α for the

upwind and downwind run occurs for waves of frequency 0.100 cps and 0.092 cps, respectively. The phase speeds of these waves are 30 and 33 knots, respectively. It is an interesting coincidence that the average wind speeds from the plane were 30 knots upwind and 33 knots downwind. While it is tempting try to relate these seemingly coupled facts, it is more prudent to exercise restraint. As mentioned previously, the wind speed is not known to anywhere near the necessary accuracy. Besides, while we have of necessity assumed a geophysically constant wind field, there can be no question that the actual wind is variable. One only need look at a typical power spectrum of horizontal wind speeds to obtain a feeling for this variability. Small changes in waves and wave growth parameters, such as just inferred, are a fact of nature. For these reasons the present work can only provide a type of averaged look at the processes of wave generation.

In comparing the observed α's with those predicted by Phillips' theory, (Section 2.0), it is necessary to estimate the three dimensional spectrum of atmospheric pressure fluctuations, $P(\vec{k}, \sigma)$, since it can be shown (Hasselmann, 1960) that

$$\alpha = 4\pi^3 k \sigma^3 / \rho \omega_g^2{}^3 \qquad P(\vec{k}, \sigma).$$

Recent work by Priestley (1965) provides the essentials for such an estimate. The applicability of Priestley's results was first realized and used by Snyder and Cox, (1966) to partially confirm Phillips (1957) theory. However, their results are restricted to one wave length and to one direction. The general evaluation of α (suggested by Snyder in a personal communication) in terms of frequency and direction is given in detail by Barnett (1966) and only the results of this evaluation are presented here. The spectrum $P(k, \sigma)$ is given by

$$P(\vec{k}, \sigma) = \frac{1}{(2\pi)^3} \int_{-\infty}^{\infty} d\vec{\eta} \, d\tau \quad R(\vec{\eta}, \tau) \cos(\vec{k} \cdot \vec{\eta} + \sigma \tau)$$

where $\vec{\eta}$ is a horizontal distance vector, τ is a lag time, and $R(\vec{\eta}, \tau)$ is the correlation function for the static pressure fluctuations. Priestley's work essentially allows one to make an empirical representation of the integrand. Direct integration then yields $P(\vec{k}, \sigma)$ in closed form. One problem arises in that the expression for $P(\vec{k}, \sigma)$ has a turbulence scaling factor in it. From Priestley's data, taken for low wind speeds over closely mowed grass, this scaling factor was found by Snyder & Cox to be proportional to approximately the fourth power of the wind speed. With such a power law it is possible to extrapolate to higher wind speeds, provided one assumes that the nature of the turbulent pressure fluctuations was similar during his experiment and ours. However, first estimates of α using such a representation for the scale factor gave values that were lower than observation by a factor of approximately 50. The fact that a difference existed was no real surprise, but it was a bit of a shock to see such a large difference. A small amount of reflection on the matter, however,

indicates that one would have to be extremely fortunate to extrapolate from the conditions under which Priestley took his limited data to those of high wind speed, a very rough, free water surface, and strong atmospheric instability. In order to compare the theory of Phillips' with measurement, then, it has been necessary to multiply all theoretical values of α by a constant factor in order to bring their magnitudes up to those observed. It should be pointed out that while such multiplication changes the magnitude, it does not affect the functional form of α. Hence, the shape of the curves shown in Figure 15 are presumably independent of the scaling factor.

The values of wind speed used to evaluate α were 30 knots upwind and 33 knots downwind. These values were selected because, not only do they give the best agreement between theory and observation, but also the wind is not known to within the limits implied by these choices. In lieu of more exact wind measurements, then, these selections allow the fairest test of the theory.

The comparison between the theoretical and observed values appears to be good. The agreement worsens with increasing frequency, but this is accounted for by an increase in the signal to noise ratio for these frequencies. From equation (4) it will be seen that the addition of noise to F causes an overestimate of α. The results are still considered quite reasonable. If, in addition to the present favorable results, one considers those obtained by Snyder and Cox (1966), it seems not unreasonable to say that a number of the original aspects of Phillips' theory have been verified. Some uncertainty must remain though, for there are still too many loop holes (scaling factor, wind speed, and Section 7.2.3) to allow an "absolute confirmation".*

7.2.3 Exponential Wave Growth

The estimates of the parameter of exponential wave growth, β, are shown on Figure 16 for both runs and all directional assumptions. That the estimates of β have little dependence on the form of K is somewhat obscured by the fact that the data from the two runs are not as similar as one would like. There are at least two possible explanations for this apparent result:

(i) The data upon which the lowest frequency estimates of β are based is rather scattered. One could put a straight line ($\beta = 0$) through the data and obtain almost as good a fit since α is but slightly affected and β is small anyway. For the higher frequency estimates of β (on the upwind run) the higher signal-to-noise ratio will cause lower estimates for reasons discussed in the following paragraph. Hence, the apparent near constant value of β with frequency.

---

*It has been rumored that such a thing does exist in geophysics.
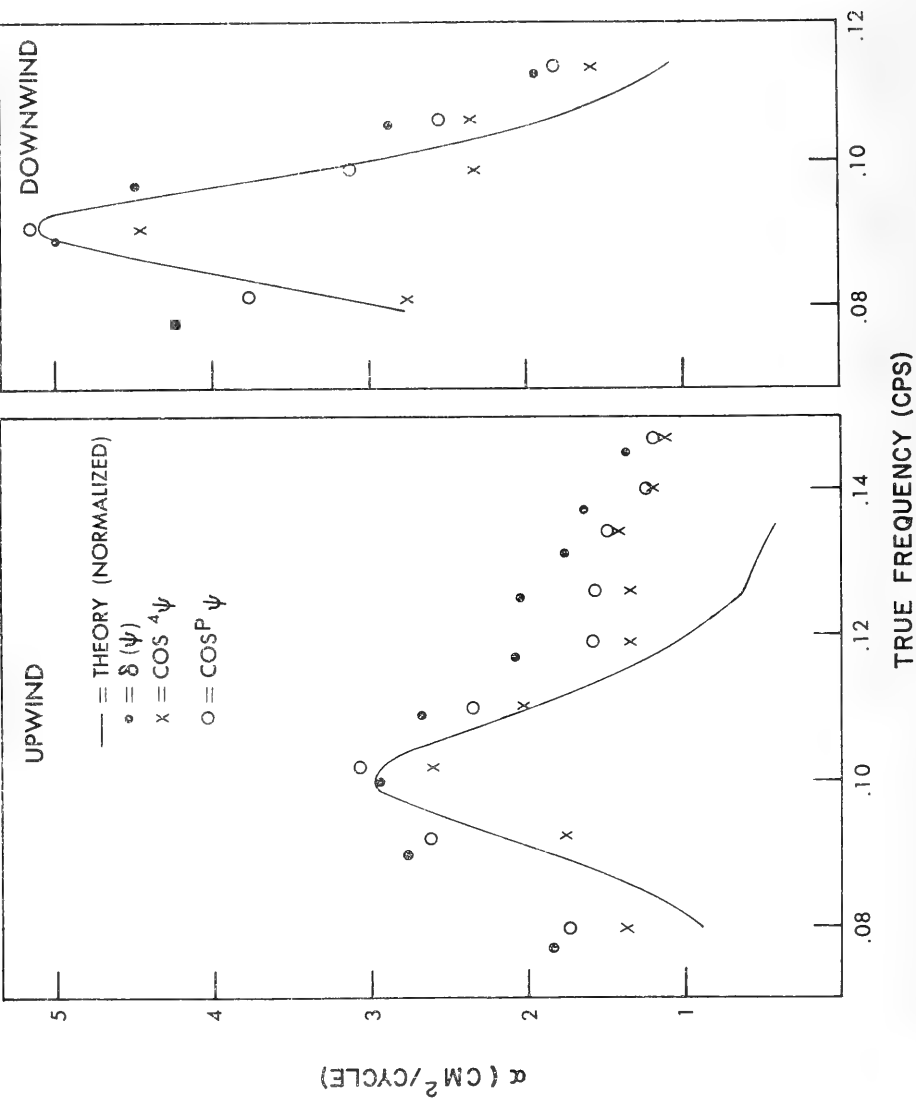
FIGURE 15. LINEAR GROWTH PARAMETER α: MEASUREMENT VERSUS THE NORMALIZED THEORETICAL PREDICTIONS OF PHILLIPS (1957).

42
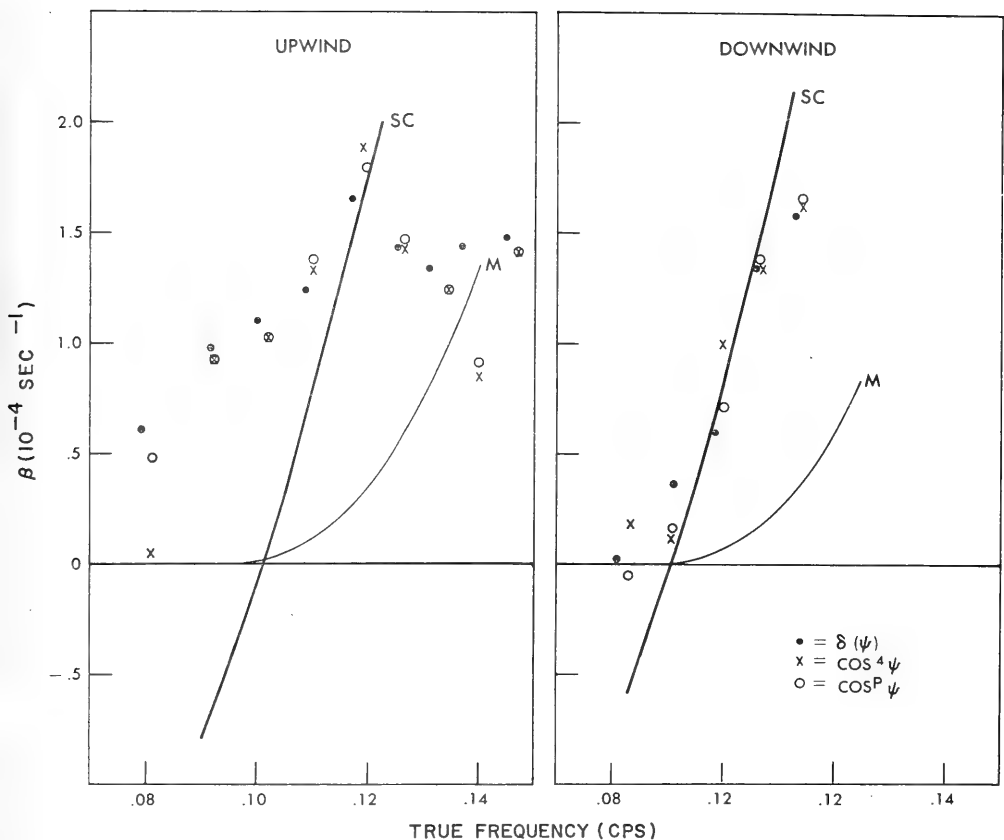
FIGURE 16. EXPONENTIAL GROWTH PARAMETER β : MEASUREMENT
VERSUS THEORY. CURVE MARKED "M" IS PREDICTED BY
MILES (1957) WHILE THE LINE "SC" IS FROM THE EMPIRICAL
RELATION OF SNYDER AND COX(1966).

(ii) One can also account for the result by allowing the wind near the coast to either drop on the upwind run or be higher for the downwind run. Such wind changes would induce either more or less (even negative) curvature, respectively, to the growth curves. Since β is essentially a measure of this curvature, the result could be as shown on Figure 16. Please note that such wind changes will be most dramatically visible in estimates of β but significantly less apparent in estimates of α and in the qualitative description of the general spectral field.

The aforegoing discussion serves to re-emphasize the fact that the numerical estimates of β , and to a lesser extent α , should be considered as order of magnitude values.

Taking into consideration the previous remarks, it is of interest to compare theory and observation. The predictions of the theory of Miles are shown in Figure 16 by the curve designated M . It is clear that this predicted curve is in agreement with none of the data. A similar conclusion about Miles' theory was reached by Snyder and Cox (1966). The other curve shown on Figure 16 (labeled SC) is an empirical relation for β suggested by those authors on the basis of this data and is defined for the case of waves travelling downwind by

$$\beta = 2 \pi \text{ sf } (W/c - 1) \tag{15}$$

where s is the ratio of the densities of air and sea water and W is the wind at a critical wave length above the mean sea surface. Neglecting the upwind run, it must be admitted that the agreement between measurement and the predictions of (15) is quite remarkable. This cannot be construed as a verification, but it does strongly suggest that there may be a good deal of physical truth in the apparently simple relation.

One of the features of Figure 16 which seems particularly significant is the fact that β is positive for waves travelling at phase speeds equal to or greater than the wind speed. Such a result seems contrary to the predictions of most instability theories. One possible explanation of this result has been given by O. M. Phillips (personal communication and in press).* Briefly, he proposes that β is the sum of two different physical processes which are acting on the wave regime. The first is identical with that proposed by Miles (1957). The second, however, is an induced effect arising from the undulatory turbulent flow over the waves. For waves travelling at or faster than the wind speed, the Miles "critical layer", or "matched layer" as Phillips calls it, contributes little or no momentum to the waves. The contribution from the undulatory turbulent flow, however, is not insignificant and, hence, now dictates the sign and magnitude of β . For a more detailed discussion of the entire concept the reader is referred to Phillips' forthcoming work.

*We are very much indebted to Professor Phillips for making preliminary details of his new theory available to us.

44

7.2.4 The Transition between Linear and Exponential Growth

Of considerable interest is the transition distance at which the processes
of linear growth and exponential growth are equal ($\alpha = \beta$ F). As postualted by
Phillips and Katz (1961), this is the fetch distance required for a particular spectral
component to occupy the steep forward face of the energy spectrum. The point has
arisen as to how good an assumption this is. To answer this question we have used
Figure 16 and the closed form solution of (4) for the downwind component to arrive
at estimates of the transition distance. These were then compared with the fetch
distances shown on Figure 17 (to be discussed in the next paragraph). The result was
that in 11 out of 13 estimates the fetch distance was roughly 2 to 4 times greater than
the transition distance. Snyder and Cox found a typical factor of 7 although their
data was not particularly suited to making the estimate. At any rate, it would appear
that the transition distance is not equivalent to the fetch distance.

The estimates of fetch distances obtained from the present data are shown in
Figure 17, a representation which is similar to that used by Phillips and Katz. Also
shown on this Figure are the measurements of Burling (1955), Kinsman (1960), and
Snyder and Cox (1966). The distances are given in numbers of wave lengths (fetch
(x)/ wavelength (L)) versus wave speed (c) over wind speed (W)the latter measured at a
height of one wave length. The wind speed actually used in Figure 17 is an average
of values observed by the aircraft, for there is no desire on the part of the authors to
extend the logrithmic profile to the heights required. The uncertainty in the wind
speed is thought to be of order 10 percent, which does not materially affect the results.

It will be seen that most of the data fits well together. The data are generally
not in agreement with the theoretical curves of Phillips and Katz (not shown) which
were derived from the theory of Miles (1957). However, the 1961 work of Phillips
and Katz has been amended by Phillips (personal communication) so that there is now,
at least, a qualitative agreement between theory and observation.. It will be inter-
esting to compare the quantitative details of Phillips' forthcoming work with the data
of Figure 17. Finally, the data shown on Figure 17 lend support to the contention of
Snyder and Cox that there is a universal relation between the fetch distance (measured
in wavelengths) at which a component occupied the "steep" forward face of the
spectrum and the wind speed measured in units of phase velocity.

7.3   Wave Dissipation

A detailed attempt to account for the limitations of wave growth as observed
in this experiment will not be undertaken. Instead, only the end result, the equil-
ibrium range of the wave spectrum, will be discussed. As mentioned in Section 7.1,
(iii), spectral components with frequencies somewhat higher than the wind frequency
(f_w) seem to grow past or "overshoot" their eventual equilibrium value. This fact is
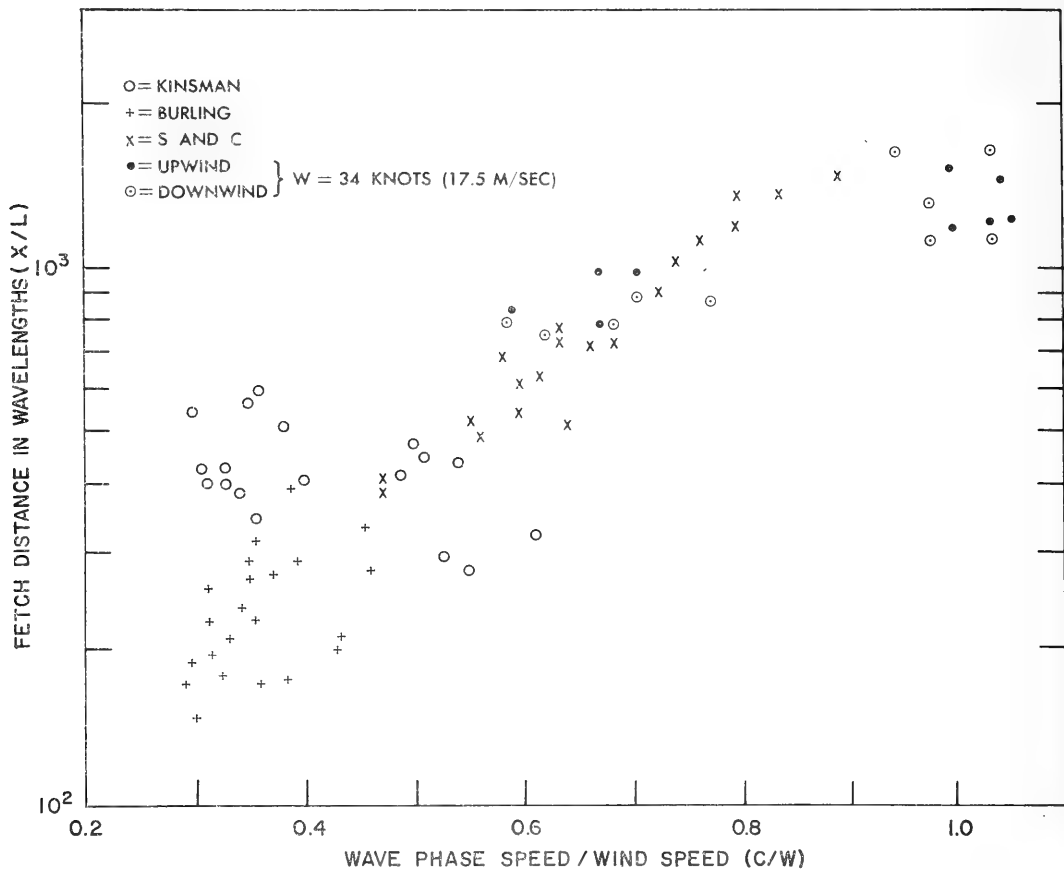
FIGURE 17. FETCH DISTANCES (EXPRESSED IN WAVE LENGTHS) AT WHICH
A COMPONENT OCCUPIES THE STEEP FORWARD FACE OF THE
SPECTRUM. ALSO SHOWN ARE THE RESULTS OF OTHER WORKERS.
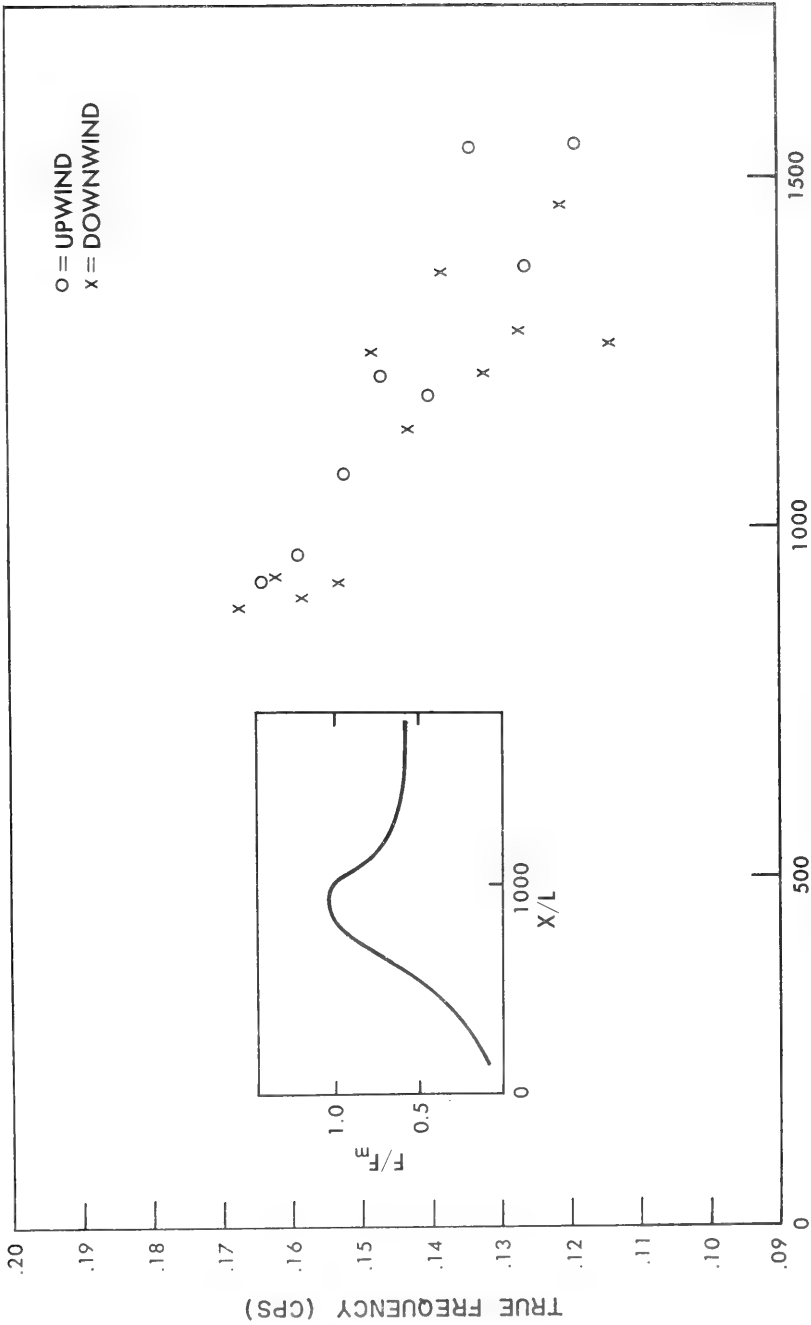
FETCH DISTANCE IN WAVELENGTHS AT WHICH F_m OCCURS (X / L)

FIGURE 18. THE "OVERSHOOT" EFFECT AND THE OCCURRENCE OF SPECTRAL COMPONENT MAXIMA IN WAVE LENGTHS FROM THE COAST.

illustrated in the inset of Figure 18 where a schematic spatial history of a spectral component is presented in non-dimensional form. The abscissa is distance downwind in wave lengths and the ordinate is the value of the component, F, at a given x divided by the maximum value, F_m, that the component achieves throughout its spatial history.

The major portion of Figure 18 shows the number of wave lengths (x/L) from the leeward fetch edge at which F_m occurs for the various frequencies. The data shown for the downwind run have neglected the near zone peak area previously mentioned. Data for only the K_3 directional assumption are presented but either of the other two spreading factors would have served as well. While there is some scatter in the data, it appears that high frequency components will reach their maximum value in fewer wave lengths than the longer, lower frequency waves.

It is informative to investigate the correspondence of the observations with proposed frequency power law formulations of the equilibrium range. Figure 19 is a log-log plot of wave frequency f versus F_m, the maximum spectral value. Only upwind values of F_m have been used. Also included in the figures are estimates, obtained through averaging, of the eventual equilibrium value F_e for both runs.* While neither of the exponents of the estimated best fit lines can be considered as precise, the relative difference between the two lines is significant. A difference of this magnitude occurs for all directional assumptions.

Whatever the ultimate cause of the "overshoot" effect, it does seem to present a possible explanation to the controversy over the form of the representation used to describe the equilibrium range of the wave spectrum. Depending on the experimental design, the amount of data taken and the frequency range considered, it would be possible to bias the results inadvertently toward either higher or lower estimates of a pure power law exponent. It is reasonable to suggest that an explanation such as given in 7.1, and a representation of the form (14) are required to more fully describe the establishment and maintenance of spectral equilibrium.

8.0 CONCLUSIONS

By using a modified airborne radar altimeter and subsequently solving a Fredholm integral equation of the first kind, it has been possible to obtain sequential estimates of fetch limited wave spectra. Since these spectra were representative of fetch distances from 3 to 190 nautical miles, it was possible to simultaneously follow the development of a number of spectral components from their very beginnings to their final, fully developed state. Although this data was taken under but one typical wind condition, it still provides unique insights into the processes of wave generation and dissipation. The more important results of this paper are summarized below:

(i) The peak of the spectrum moves toward lower frequencies with distance from

*It turns out that F_e/F_m for both runs is between .35 to .75 with the data being badly scattered.
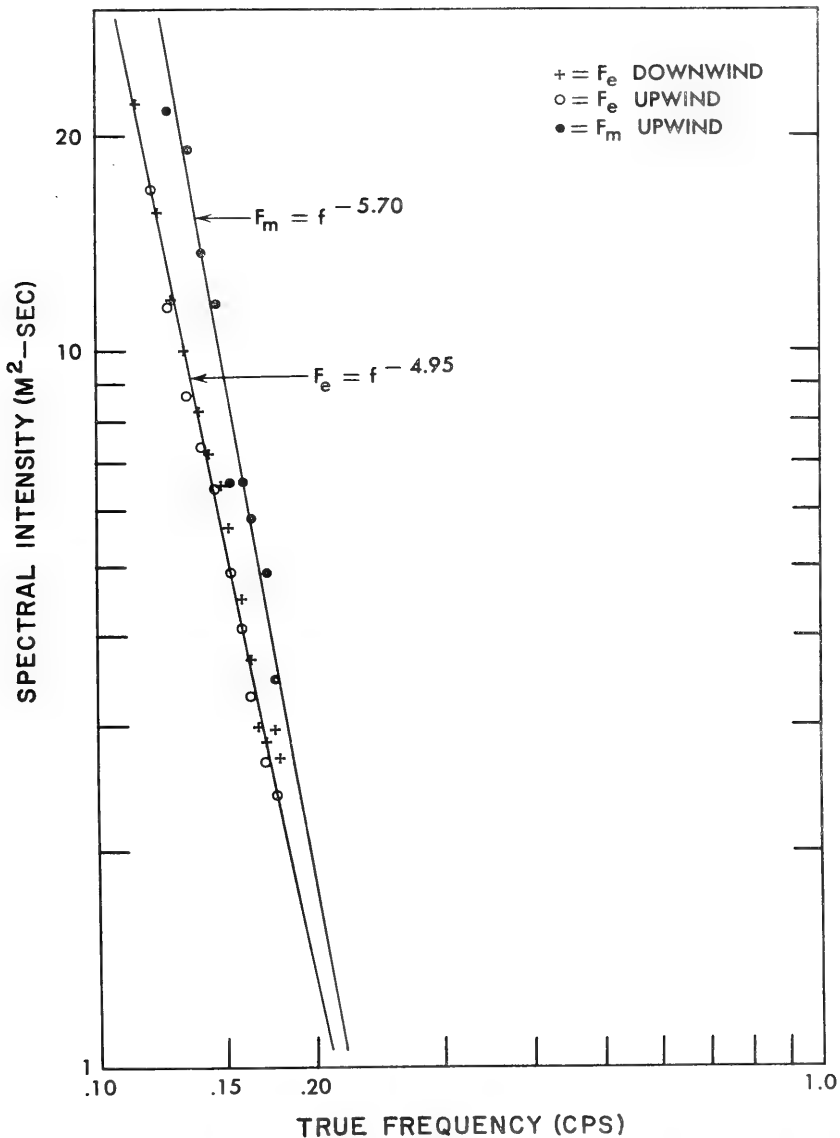
FIGURE 19. LOG-LOG PLOT OF F_m AND F_e VERSUS WAVE FREQUENCY.

the leeward fetch edge.

(ii) Energy was being transmitted to the entire frequency range of the spectrum simultaneously.

(iii) A particular spectral component, of frequency somewhat higher than the wind frequency, grows until it has occupied the position of the spectral peak. After that time (distance) the component does not maintain its maximum energy, but instead, loses energy until it reaches a final equilibrium value which is between 30-70% of the maximum. This indicates that a simple power law description of the wave breaking region (generally called the equilibrium range) may not be adequate. A more complicated relation, such as (14), suggesting a connection between wave breaking and the position of the spectral peak seems called for.

(iv) The observed rates of spectral growth are in substantial agreement with the observations of Snyder and Cox (1966). This agreement lends considerable support to the conclusions drawn by those authors concerning the wind generation of ocean waves.

(v) The predictions of Phillips' (1957) theory concerning wave generation by turbulent atmospheric pressure fluctuations are in good accord with the observed growth rates. The data suggest, however, that under unstable atmospheric conditions, the pressure spectrum scaling factor (Priestley, 1965) must be increased by several orders of magnitude over that expected for near-neutral conditions in order to make the theory compatible.

(vi) The predictions of Miles' (1957) theory concerning wave growth by an instability mechanism are not in agreement with present data. This reaffirms the conclusion of Snyder and Cox, that the instability which is present appears to be an order of magnitude stronger than predicted by Miles. It is interesting, and perhaps suggestive, that the "simple" empirical relation, (15), proposed by those authors is in good agreement with the downwind data.

(vii) It is of considerable significance that the coefficient of exponential growth, β (Figure 16), is positive for waves whose phase speeds are equal to or greater than the wind speed.

(viii) Estimates of the fetch distance where a component occupies the steep forward face of the spectrum are in good agreement with other data. The observations also indicate that these fetch distances are 2 to 4 times greater than the transition distance as defined by Phillips and Katz (1961).

REFERENCES

Baer, L., 1962, "An Experiment in Numerical Forecasting of Deep Water Ocean Waves," Lockheed Missile and Space Company, Report 801296, L. M. S. C., Sunnyvale, California.

Barnett, T. P., (in preparation), "On the Generation, Dissipation, and Prediction of Ocean Wind Waves", Scripps Institution of Oceanography Doctoral Thesis.

Blackman, R. B., and J. W. Tukey, 1958, The Measurement of Power Spectra, New York, Dover Press.

Burling, R. W., 1955, "Wind Generation of Waves on Water", Ph.D. Dissertation, Imperical College, Clair, of London, p. 181.

Cartwright, D. E., 1963, "The Use of Directional Spectra in Studying the output of a Wave Recorder on a Moving Ship", Ocean Waves Spectra, Prentice-Hall, Inc., Englewood Cliffs, New Jersey., pp. 203-218.

Cote, L. J. and others, 1960, "The Directional Spectrum of a Wind Generated Sea as Determined from Data Obtained by the Stereo Wave Observation Project", Met. papers, 2, No. 6, New York University, New York, p. 87.

DeLeonibus, P. S., (in preparation), "Measurements of Momentum Flux at Argus Island Tower, Bermuda".

Groves, G. W. and J. Melcer, 1961, "On the Propagation of Ocean Waves on a Sphere", Geo. Int., 1, 4, pp. 77-93.

Hasselman, K., 1960, "Grundgleighungen der Seegangsvoraussage", Shiffstechnik, 1, pp. 191-195.

Hidy, G. M., 1965, "The Growth of Wind Waves on Water in a Channel", NCAR Manuscript No. 66, p. 18.

Kinsman, B., 1960, "Surface Waves at Short Fetch and Low Wind Speed -- A Field Study", Technical Report No. 19, Chesapeake Bay Inst., The John Hopkins University., p. 169.

Longuett-Higgins, M. S. and others, 1963, "Observations of the Directional Spectrum of Sea Waves using the Motions of a Floating Buoy", Ocean Wave Spectra, Prentice-Hall, Inc., Englewood Cliffs, New Jersey, pp. 111-132.

Miles, J. W., 1957, "On the Generation of Surface Waves by Shear Flows", Part 1, J. Fluid Mechanics, 3, pp. 185-204.

Munk, W. H. and others, 1963, "Directional Recording of Swell from Distance Storms", Phil Trans. Roy. Soc., 255, 1062, p. 538.

Neumann, G. and W. J. Pierson, 1963, Ocean Wave Spectra, op.cit., p. 13.

Phillips, O. M., 1957, "On the Generation of Waves by Turbulent Wind", J. Fluid Mechanics, 2, pp. 417-445.

Phillips, O. M., 1958a, "Wave Generation by Turbulent Wind over a Finite Fetch", Proceeding of the third U. S. National Congress of Applied Mechanics, Am. Soc. Mech. Eng., pp. 785-789.

Phillips, O.M., 1958b, "The Equilibrium Range in the Spectrum of Wind Generated Waves", J. Fluid Mechanics, 4, pp. 426-434.

Phillips, O. M. and E. J. Katz, 1961, "Low Frequency Components of the Spectrum of Wind Generated Waves", J. Mar. Res., 19, pp. 57-69.

Phillips, O.M., 1963, Prepared comments, Ocean Wave Spectra, Op.Cit., p. 34.

Pierson, W. J. and others, 1955, "Observing and Forecasting Ocean Waves", H. O. Publication Number 603, U. S. Navy Hydrographic Office, p. 284.

Pierson, W. J. and L. Moskowitz, 1963, "A Proposed Spectral Form for Fully Developed Wind Seas Based on the Similarity Theory of F. A. Kitzigorodskii", Geophysical Sciences Lab. Report 63-12, New York University, School of Engineering and Science.

Priestley, J. T., 1965, "Correlation Studies of Pressure Fluctuations on the Ground Beneath a Turbulent Boundary Layer", "National Bureau of Standards Report 8942 ", National Bureau of Standards, p. 92.

Redish, K. A., 1961, An Introduction to Computational Methods, John Wiley and Sons, Inc., New York, New York, p. 211.

Snyder, R. L., 1965, "The Wind Generation of Ocean Waves", Ph.D. dissertation, University of California, San Diego, pp. 393.

Snyder, R. L. and C. S. Cox, 1966, "A Field Study of the Wind Generation of Ocean Waves", J. Mar. Res.

St. Denis, M. and W. J. Pierson, 1953, "On the Motions of Ships in confused seas", Trans. Soc. Nav. Arch. and Mar. Eng., <u>61</u>, pp. 332-357.

APPENDIX   A

DISTANCE (N. M.)

57

F (M_a^2 -SEC.)

DISTANCE (N.M.)

f = 0.108
K ~ $COS^P\psi$

f = 0.100
K ~ $COS^P\psi$

f = 0.108
K ~ $COS^4\psi$

f = 0.100
K ~ $COS^4\psi$

f = 0.108
K ~ $6(\psi)$

f = 0.100
K ~ $6(\psi)$

DISTANCE (N.M.)

59

F (M.² -SEC.)

DISTANCE (N.M.)

61

DISTANCE (N.M.)

62

U. S. Naval Oceanographic Office
ON THE INTERPRETATION OF FETCH-
LIMITED WAVE SPECTRA AS MEASURED BY
AN AIRBORNE SEA-SWELL RECORDER, by
T. P. Barnett and J. C. Wilkerson, May 1967,
62 pages, 26 figs., 2 tables (TR-191)

References pp. 51-53

Fetch limited wave spectra that have been
generated by a steady wind were sequencially
measured using an airborne sea-swell recorder.
From this data it was possible to estimate rates
of growth for various components of the spectrum.
These growth rates are compared with the theories
of Phillips (1957) and Miles (1959) and with the
measurements of Synder & Cox (1966). An unex-
pected result of the analysis was that waves some-
times grow past or "overshoot" their eventual
equilibrium energy value.

1. On the Interpretation of Fetch-
   Limited Wave Spectra as
   Measured by an Airborne Sea-
   Swell Recorder.
2. Fetch Limited Wave Spectra as
   Measured by an Airborne Sea-
   Swell Recorder, on the Inter-
   pretation of.
   i. title: On the Interpretation of
      Fetch-Limited Wave Spectra as
      Measured by an Airborne Sea-
      Swell Recorder.
   ii. authors: T.P. Barnett and J.C.
       Wilkerson
   iii. TR-191

U. S. Naval Oceanographic Office
ON THE INTERPRETATION OF FETCH-
LIMITED WAVE SPECTRA AS MEASURED BY
AN AIRBORNE SEA-SWELL RECORDER, by
T. P. Barnett and J. C. Wilkerson, May 1967,
62 pages, 26 figs., 2 tables (TR-191)

References pp. 51-53

Fetch limited wave spectra that have been
generated by a steady wind were sequencially
measured using an airborne sea-swell recorder.
From this data it was possible to estimate rates
of growth for various components of the spectrum.
These growth rates are compared with the theories
of Phillips (1957) and Miles (1959) and with the
measurements of Synder & Cox (1966). An unex-
pected result of the analysis was that waves some-
times grow past or "overshoot" their eventual
equilibrium energy value.

1. On the Interpretation of Fetch-
   Limited Wave Spectra as
   Measured by an Airborne Sea-
   Swell Recorder.

2. Fetch Limited Wave Spectra as
   Measured by an Airborne Sea-
   Swell Recorder, on the Inter-
   pretation of.

   i.   title: On the Interpretation of
        Fetch-Limited Wave Spectra as
        Measured by an Airborne Sea-
        Swell Recorder.

   ii. authors: T.P. Barnett and J.C.
        Wilkerson

   iii. TR-191

U. S. Naval Oceanographic Office
ON THE INTERPRETATION OF FETCH-
LIMITED WAVE SPECTRA AS MEASURED BY
AN AIRBORNE SEA-SWELL RECORDER, by
T. P. Barnett and J. C. Wilkerson, May 1967,
62 pages, 26 figs., 2 tables (TR-191)

References pp. 51-53

Fetch limited wave spectra that have been
generated by a steady wind were sequencially
measured using an airborne sea-swell recorder.
From this data it was possible to estimate rates
of growth for various components of the spectrum.
These growth rates are compared with the theories
of Phillips (1957) and Miles (1959) and with the
measurements of Synder & Cox (1966). An unex-
pected result of the analysis was that waves some-
times grow past or "overshoot" their eventual
equilibrium energy value.

1. On the Interpretation of Fetch-
   Limited Wave Spectra as
   Measured by an Airborne Sea-
   Swell Recorder.

2. Fetch Limited Wave Spectra as
   Measured by an Airborne Sea-
   Swell Recorder, on the Inter-
   pretation of.

   i.   title: On the Interpretation of
        Fetch-Limited Wave Spectra as
        Measured by an Airborne Sea-
        Swell Recorder.

   ii. authors: T.P. Barnett and J.C.
        Wilkerson

   iii. TR-191

U. S. Naval Oceanographic Office
ON THE INTERPRETATION OF FETCH-
LIMITED WAVE SPECTRA AS MEASURED BY
AN AIRBORNE SEA-SWELL RECORDER, by
T. P. Barnett and J. C. Wilkerson, May 1967,
62 pages, 26 figs., 2 tables (TR-191)

References pp. 51-53

Fetch limited wave spectra that have been
generated by a steady wind were sequencially
measured using an airborne sea-swell recorder.
From this data it was possible to estimate rates
of growth for various components of the spectrum.
These growth rates are compared with the theories
of Phillips (1957) and Miles (1959) and with the
measurements of Synder & Cox (1966). An unex-
pected result of the analysis was that waves some-
times grow past or "overshoot" their eventual
equilibrium energy value.

1. On the Interpretation of Fetch-
   Limited Wave Spectra as
   Measured by an Airborne Sea-
   Swell Recorder.

2. Fetch Limited Wave Spectra as
   Measured by an Airborne Sea-
   Swell Recorder, on the Inter-
   pretation of.

   i.   title: On the Interpretation of
        Fetch-Limited Wave Spectra as
        Measured by an Airborne Sea-
        Swell Recorder.

   ii. authors: T.P. Barnett and J.C.
        Wilkerson

   iii. TR-191

U. S. Naval Oceanographic Office
ON THE INTERPRETATION OF FETCH-
LIMITED WAVE SPECTRA AS MEASURED BY
AN AIRBORNE SEA-SWELL RECORDER, by
T. P. Barnett and J. C. Wilkerson, May 1967,
62 pages, 26 figs., 2 tables (TR-191)

References pp. 51-53

Fetch limited wave spectra that have been
generated by a steady wind were sequencially
measured using an airborne sea-swell recorder.
From this data it was possible to estimate rates
of growth for various components of the spectrum.
These growth rates are compared with the theories
of Phillips (1957) and Miles (1959) and with the
measurements of Synder & Cox (1966). An unex-
pected result of the analysis was that waves some-
times grow past or "overshoot" their eventual
equilibrium energy value.

1. On the Interpretation of Fetch-
   Limited Wave Spectra as
   Measured by an Airborne Sea-
   Swell Recorder.

2. Fetch Limited Wave Spectra as
   Measured by an Airborne Sea-
   Swell Recorder, on the Inter-
   pretation of.

   i.   title: On the Interpretation of
        Fetch-Limited Wave Spectra as
        Measured by an Airborne Sea-
        Swell Recorder.

   ii. authors: T.P. Barnett and J.C.
        Wilkerson

   iii. TR-191

DOCUMENT CONTROL DATA - R&D

(Security classification of title, body of abstract and indexing annotation must be entered when the overall report is classified)

1. ORIGINATING ACTIVITY (Corporate author)	2a. REPORT SECURITY CLASSIFICATION
U. S. Naval Oceanographic Office	Unclassified
	2b. GROUP

3. REPORT TITLE

On the Interpretation of Fetch-Limited Wave Spectra as Measured by an Airborne Sea-Swell Recorder.

4. DESCRIPTIVE NOTES *(Type of report and inclusive dates)* This report makes up a portion of the principle author's Ph.D thesis — submitted to Scripps Institution of Oceanography.

5. AUTHOR(S) *(Last name, first name, initial)*

Barnett, T. P. and J. C. Wilkerson

6. REPORT DATE	7a. TOTAL NO. OF PAGES	7b. NO. OF REFS
May 1967	71	27

8a. CONTRACT OR GRANT NO.	9a. ORIGINATOR'S REPORT NUMBER(S)
Not applicable	
b. PROJECT NO.	TR-191
Not applicable	
c.	9b. OTHER REPORT NO(S) (Any other numbers that may be assigned this report)
d.	None

10. AVAILABILITY/LIMITATION NOTICES

Qualified users may obtain copies of this report from DDC.

11. SUPPLEMENTARY NOTES	12. SPONSORING MILITARY ACTIVITY
None	U. S. Naval Oceanographic Office

13. ABSTRACT

A section of sea surface that had been subjected to a constant, offshore wind was profiled using an airborne radar wave profiler. The profiles extended from the coast out a distance of 190 nautical miles. From this data estimates of the spectrum of encounter of the sea surface were obtained for a number of different fetch lengths. By solving a singular Fredholm integral equation of the first kind, it was possible to retrieve the true wave spectrum as a function of fetch length. Spectral growth curves were then obtained and analyzed in light of recent theories of wave generation. The data lend support to the previous conclusions of Snyder and Cox (1966) regarding two recent theories of wave generation. Specifically, the data are consistent with the "resonance" theory of wave growth (Phillips, 1957), but at the same time suggests that wave growth through an instability mechanism (Miles, 1957) is yet to be understood. One of the most significant results of this study was that higher frequency waves grow past or "overshoot" their eventual equilibrium energy value. After "overshooting" they then rapidly decay back to an equilibrium range.

DD FORM 1 JAN 64 1473